nagra.

Arbeitsbericht NAB 22-23

Diffusion Experiments on Clayey Rock Samples from Nagra's Deep Drilling Campaign as Part of a Benchmarking Study

March 2022

L. Van Laer, M. Aertsens,
N. Maes, M. Glaus & L. Van Loon

National Cooperative
for the Disposal of
Radioactive Waste

Hardstrasse 73
P.O. Box 280
5430 Wettingen
Switzerland
Tel. +41 56 437 11 11

www.nagra.ch

nagra.

Arbeitsbericht NAB 22-23

Diffusion Experiments on Clayey Rock Samples from Nagra's Deep Drilling Campaign as Part of a Benchmarking Study

March 2022

L. Van Laer, M. Aertsens,
N. Maes, M. Glaus & L. Van Loon

SCK CEN

KEYWORDS

Diffusion, effective diffusion, clay rocks, Opalinus Clay, Trüllikon-1-1, HTO, Cl, Na, benchmark study, diffusion parameters, capacity factors, SCK CEN

National Cooperative for the Disposal of Radioactive Waste

Hardstrasse 73
P.O. Box 280
5430 Wettingen
Switzerland
Tel. +41 56 437 11 11

www.nagra.ch

Nagra Arbeitsberichte ("Working Reports") present the results of work in progress that have not necessarily been subject to a comprehensive review. They are intended to provide rapid dissemination of current information.
This report was prepared on behalf of Nagra. The viewpoints presented and conclusions reached are those of the author(s) and do not necessarily represent those of Nagra.

Abstract

This study involved diffusion experiments on a set of clay samples obtained from the ongoing deep borehole drilling campaign of Nagra as part of their site selection process. It is part of a benchmark study where SCK CEN was asked to perform diffusion studies on five core samples in collaboration with the main contractor PSI-LES in order to confirm previous findings that through-diffusion experimental measurement errors are acceptable.

Five clay plugs from the Trüllikon-1 borehole were subjected to diffusion of HTO, Cl-36 and Na-22 in synthetic pore water. The samples were taken between 870 and 940 m depth. The independently determined diffusion parameters from SCK CEN and PSI-LES confirm previously found uncertainties. The variability of the effective diffusion coefficients estimated independently by both institutes was less than a factor 2 and often even much lower. Also, the parameter estimations of the capacity factor (or porosity in case of HTO and Cl-36) agreed well. As an additional benchmark modelling exercise, the experimental datasets of HTO and Cl-36 were also fitted by the model approach of the other institute. The variability among the obtained diffusion parameters was in the same order as the variability of the independently obtained parameters (effective diffusion coefficients and capacity factors).

Table of Contents

List of Tables

List of Figures

1 Introduction

This contract work consisted of performing through-diffusion experiments at SCK CEN with HTO, Cl-36 and Na-22 on five core samples from the Trüllikon-1 borehole of Nagra, with four samples of the Opalinus Clay Formation and one from the Staffelegg Formation. This was done in close collaboration with University of Bern and PSI-LES. University of Bern was responsible for the sample selection, the sample preparation and the pore water characterisation (in order to define a recipe for the synthetic pore water). The experimental conditions and the streamlining of the experimental protocols and data treatment were done by exchange with PSI-LES.

The five clay plugs from the Trüllikon-1 borehole were taken between 870 and 940 m depth. They were subjected to diffusion of HTO, Cl-36 and Na-22 in synthetic pore water (Opalinus Clay) by PSI-LES and SCK CEN. The aim of this benchmark study was to assess the reproducibility of results when tests are done by different laboratories for (nearly) the same sample material. This is done by comparing the parameter values obtained by SCK CEN and PSI-LES using their in-house experimental and modelling methodologies for through-diffusion experiments. In this way it is possible to assess the effect of the experimental and modelling uncertainties on the uncertainty of the diffusion parameters.

After the description and interpretation of the obtained data by both institutes (parts 2 and 3), a comparison of the parameters is done in Part 4 "Benchmark study".

2 Experiments @SCK CEN

2.1 Materials & methods

2.1.1 Samples and sample preparation

The clay samples originate from cores from the Trüllikon-1 borehole. At five depths two samples next to each other were subsampled from drill cores and provided to PSI-LES and SCK CEN. The four samples taken at a depth between 870 and 903 m originate from the Opalinus Clay Formation, while the sample at 938 m is part of the Staffelegg Formation. The clay plug samples of 64 mm diameter and ± 12 – 14 mm thickness were embedded in resin by the University of Bern and distributed in vacuum sealed bags to PSI-LES and SCK CEN.

After unpacking the clay plugs outside the glovebox, they were visually inspected (pictures in order to check for possible damage). They were weighed and the diameter and thickness of the clay plugs was measured. Since the thickness of the clay plugs could vary over the plug, it was measured at 4 sides of the clay plug. The average thickness was used for the modelling.

2.1.2 Synthetic pore water

Synthetic pore water (SPW) was prepared under anaerobic conditions with degassed water inside the controlled atmosphere glovebox according to the recipe provided by PSI-LES for SPW-TRU1 used for experiments with samples from the borehole Trüllikon-1 (TRU1) (Appendix A). All chemicals used were of analytical grade or pure. The composition is given in Tab. 2-1.

Tab. 2-1: Composition of the SPW

Element	**Concentration** [M]
Na	2.44×10^{-1}
K	1.64×10^{-3}
Ca	2.22×10^{-2}
Mg	1.56×10^{-2}
Sr	2.89×10^{-4}
Cl	2.72×10^{-1}
S (as SO_4)	2.43×10^{-2}
C (as HCO_3)	4.87×10^{-4}
pH	7.68
I	0.354

The target pH value was between 7.6 and 7.8. In the glovebox the pH in the stock solution tended to increase up to 8.5 (depending on the time). Therefore, the pH of the stock solution was adapted by adding HCl aliquots (~ 5 – 50 µL HCl 1 M per liter SPW) until the pH reached again a value in the desired range every time when new outlet solutions were transferred into the vials. During the experiment there was no monitoring of the pH in order to minimize disturbance of the experiments.

2.1.3 Diffusion cells

Diffusion cells were designed (Appendix B) and manufactured in line with the provided sample size (clay rock dimensions of length L = 12 – 14 mm × diameter Ø = 62 – 64 mm and a total diameter, including the resin, of ± 94 mm) and experimental requirements. The cells are manufactured in stainless steel (316L) because of its durability and mechanical stability (vs. swelling behaviour of the clay). The cell design (Appendix A) was based on the PSI design. It consists of two-end cap flanges in which the cylindrical embedded sample is confined. The flanges have a chamber to place a porous filter disc (also made of stainless steel) which allows the circulation of SPW. The porous filter discs (Sika-R10X) with a thickness of 2 mm have an average pore diameter of 17 µm and a porosity of 43% (specifications from the supplier). These porous filter plates are in contact with channels in the flanges through which solution from the source and target reservoir is continuously pumped using a peristaltic pump.

2.1.4 Glovebox

The glovebox (MBraun MB 150 B-G) was tuned to 400 ppm CO_2 by using an inert working gas Ar containing 400 ppm CO_2, in refreshing/flushing modus. The glovebox atmosphere was monitored for oxygen with oxygen levels being on average < 1 ppm and never exceeding 5 ppm. This was checked on a daily basis by the lab technician responsible for sampling. The gas atmosphere is continuously circulated over catalyst columns to remove the oxygen. The CO_2 level was monitored manually at every sampling time with a portable CO_2 monitor, without active control/dosing of CO_2 to the target level of 400 ppm. The CO_2 level varied only between 400 and 420 ppm, and no adjustments of the CO_2 level during the course of the experiments were done. The temperature in the glovebox was monitored at every sampling time. It varied between 21 and 24 °C.

2.1.5 Diffusion measurements

Loading clay plug

After unpacking the clay plugs from the vacuum sealed bags, the clay plugs were inspected, weighed, measured (thickness & diameter) and immediately mounted between the two flanges of the diffusion cell. The exposure to air was as much as possible minimised and lasted maximum 30 minutes. The clay plug was confined between the two flanges by bolts and screws to keep a constant volume, but no special measures were taken to control the confining pressure. After mounting the clay plugs in the diffusion set-ups, the experimental set-ups were transferred into the glovebox.

Re-saturation

Prior to the diffusion experiments, the clay plugs were re-saturated with SPW during 6 weeks. The diffusion cells were turned over regularly to remove air bubbles until bubbles were no longer observe. The SPW solution (40 mL) was used to re-saturate/equilibrate source and target side at the same time and was refreshed every week. The composition was analysed in order to check if the pore water chemistry was stable before starting the diffusion experiments.

Diffusion experiments

The experimental set-up of the through-diffusion experiment is given in Fig. 2-1. The diffusion cell is at one side connected with the source reservoir (labelled SPW) and at the other side with the target reservoir (unlabelled SPW). The source reservoir (± 100 mL) contained SPW (equilibrated with the clay for a few days) labelled with the desired tracers (start activity ± 500 Bq/mL). Aliquot samples of 100 µL were taken every week. In the first diffusion experiments with HTO and Cl-36 one aliquot was sampled each time, while in the second diffusion experiment with Na-22, duplicate samples were taken. The target reservoir (± 15 mL) contained unlabelled SPW and was refreshed every day within the first nine days and then at a sampling regime of 2/2/3 days (Mon-Wed-Fri) in order to keep the concentration low and constant to achieve the desired boundary conditions for modelling. Subsamples of 4 or 5 mL were analysed. The weight of the samples was recorded on an analytical balance with a resolution of 0.0001 g. However, for the samples of the source reservoir fixed volumes were used to calculate the concentrations (Bq/mL) in the source reservoir instead of the volumes based on the weight, because the uncertainty of weighing the small sample volumes was too high when weighing them in the glovebox (less stable readings) or evaporation could take place during storing and transferring them out of the glovebox.

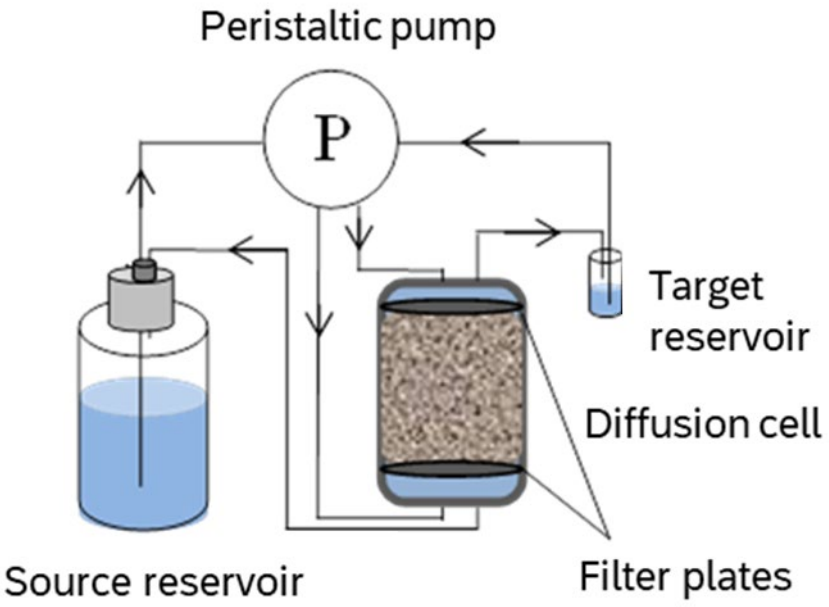

Fig. 2-1: Schematic presentation of the through-diffusion experimental set-up

The through-diffusion experiments were performed in VC-CC conditions, meaning variable concentration (VC) in the source reservoir (large volume), while keeping constant concentration (CC) at the target reservoir by using a small volume that is replaced frequently (every 2 – 3 days) (quasi-constant concentration)[1]. Both reservoirs were sampled during 2 – 3 months until a slowly decreasing flux for at least 10 data points was achieved.

A peristaltic pump (Ismatec IPC-12) was used to continuously pump the solutions at the up- and downstream sides through the filter plates. In the first series of diffusion experiments (HTO and Cl-36) there was a pump failure between day 21 and 31. Continuously pumping was no longer feasible, but the solutions could still be pumped at regular times for a time interval of 5 – 10 minutes.

In a first series, diffusion experiments were performed with HTO and Cl-36, which decay both by beta emission. Their distinct decay energy difference (18.6 keV for HTO versus 710 keV for Cl-36) allowed to separate their spectra using liquid scintillation counting. The diffusion of Na-22 was performed in a second step, since Na-22 decay by beta emission at a characteristic energy of 511 keV is interfering with the measurement of Cl-36. The diffusion experiments with Na-22 were started after the experiment with HTO and Cl-36 (without out-diffusion of the other tracers). Na-22 also emits a characteristic gamma ray at 1'275 keV, hence gamma measurement was used for the follow up of the Na-22 diffusion as this is not interfered by the beta emission of HTO or Cl-36.

There were no specific measures taken to avoid impact of micro-organisms.

2.1.6 Water content measurements

At the end of the experiments, the clay samples were removed from the diffusion set-ups, dipped dry and the wet weight was determined. Thereafter, they were put in an oven at 105 °C until constant weight in order to determine the water content as proxy for the full porosity.

2.1.7 Analytics

Pore water chemistry

The chemical composition of the SPW was checked both before and after the re-saturation and after executing the diffusion experiments. The inactive samples were analysed by ICP-OES (Varian 720-ES ICP-OES, Agilent, Santa Clara, California, USA) for the cations and by IC (Dionex ICS2000) for the anions at the Geology Department KU Leuven). The inorganic carbon was analysed by the in-house TIC/TOC analyser (Shimadzu TOC-L CPH)). The active samples were analysed by ICP-OES (Thermo Scientific iCAP 7400 rad) for the cations and by IC (Thermo Scientific Dionex Aquion IonPac AS22) for the anions by SCK CEN's ISO 17025 certified Radiochemical Analysis Labs (RCA).

[1] "Source" and "target" are also referred to as "inlet" and "outlet" throughout the report.

Radio-assay

In a first series, diffusion experiments were performed with HTO and Cl-36, which decay both by beta emission. Their distinct decay energy difference (18.6 keV for HTO versus 710 keV for Cl-36) allowed to separate their spectra using liquid scintillation counting. The diffusion of Na-22 was performed in a second step, since Na-22 decay by beta emission at a characteristic energy of 511 keV is interfering with Cl-36. The diffusion experiments with Na-22 were started directly after the experiment with HTO and Cl-36 (without out-diffusion of the other tracers) Na-22 also emits a characteristic gamma ray at 1'275 keV, hence gamma measurement was used for the follow up of the Na-22 diffusion as this is not interfered by the beta emission of HTO or Cl-36.

Activity measurements of HTO and Cl-36 were performed by the in-house LSC Counter (Liquid Scintillation Counter Packard TriCarb 2100TR). Na-22 activity was measured with gamma counter (Packard Cobra Quantum gamma counter).

A comprehensive optimisation and validation study of the LSC and gamma analysis technique was carried out, including also the determination of the measurement uncertainty. The QC of the measurements consisted of:

- regular calibrations of our own LSC and gamma counter
- checks by means of standards in each measurement series
- background/blank checks and corrections

The validation/optimization studies of the different radionuclides are given in Appendix C.

2.1.8 Uncertainties

The calculation of the measurement uncertainty of the measured activities with liquid scintillation counting and gamma counting is elaborated in Appendix C.1 and C.2. For activities above 2 Bq/mL this measurement uncertainty is ~ 1%. When replicate samples are analysed, the standard deviation between the replicate samples is in general between 0.2 and 15% of the average value. For the 95% confidence interval the standard error of two replicate samples is calculated as 12.7*stdev/(√n), for three replicate samples 4.3*stdev/(√n). For the inlet concentration the error bars are taken conservatively 15% of the measured values, as for HTO and Cl-36 there were no replicate samples taken (in order to limit the decrease of the volume of the inlet reservoir).

2.1.9 Parameter estimation

The diffusion parameters of a tracer in a porous medium are the apparent diffusion coefficient D_a and the capacity factor ηR. The capacity factor ηR is the product of the accessible porosity η and the retardation factor R. During a diffusion experiment, only the product ηR can be determined, not the individual constituents η and R. For small neutral tracers, like HTO, and anions, the retardation factor R is taken equal to one (R = 1, no retardation) making that the capacity factor reduces to the accessible porosity (ηR = η). The HTO accessible porosity is also the total porosity: $\eta_{HTO} = \eta_{tot}$. For cations, the accessible porosity is taken equal to the HTO accessible porosity η_{tot}:

$$(\eta R)_{cation} = \eta_{tot} R_{cation} \quad (1)$$

Besides, the effective diffusion D_e is defined as the product of the apparent diffusion coefficient and the capacity factor:

$$D_e = \eta R\, D_a \quad (2)$$

Diffusion occurs in the clay core as well as in the filters confining this core. The way how the values of the diffusion parameters in the filters ($D_{e,f}$ and $(\eta R)_f$ in the filters vs. $D_{e,C}$ and $(\eta R)_C$ in the clay) are taken into account affects the values of the diffusion parameters in the clay. Details on the model and how the fits are performed are provided in section 7.4. The diffusion-advection equation is numerically solved with the COMSOL® software (Aertsens et al. 2017). The fit programme "dfit36_varC0_V3_met_filters_weak" allows to fit the evolution of the inlet concentration and/or the evolution of the outlet concentration and/or a tracer profile measured in the clay at the end of the experiment. Concerning the outlet concentration: it is possible to fit the evolution of (1) the measured outlet concentrations, (2) the measured outlet flux or (3) the accumulated outlet mass.

Since inlet and outlet concentration are measured as a function of time, it is obvious to fit both simultaneously, which requires "relative" fits (see Appendix D.3). In that case, fitting cumulative fits or fitting the outlet concentration leads to similar optimal values (typically differences up to 10%). We report here the results of fitting inlet and outlet concentrations simultaneously.

To fit the optimum values there are different options available as well (more details in Appendix D.1):

- All parameters (apparent diffusion coefficient in the clay, apparent diffusion coefficient in the filters, capacity factor in the clay, capacity factor in the filters) can be fitted and/or given a constant value in any combination.
- It is possible to assume the same values for the diffusion parameters in filters and in clay (apparent diffusion coefficient in the clay = apparent diffusion coefficient in the filters and capacity factor in the clay = capacity factor in the filters).
- It is possible to assume the same values for the apparent diffusion coefficients in filters and in clay, while the capacity factors in the clay and in the filters have a different value.

For the purpose of these experiments two options were used, i.e. (i) same parameters for filter and clay (F=C) and (ii) fixed filter parameters (FF). The FF option is in theory the most relevant provided that representative parameter values for the filters are available. The values used here are values obtained for HTO diffusion in filters with similar properties (ηR_f = 0.4, $D_{a,f}$ = 3.5 10^{-10} m^2/s, Aertsens et al. (2011)). For Cl-36 and Na-22, these values are not determined and hence the values for HTO were used. It must be noted that when using filters to confine clay systems, due to swelling effects, clay particles can become pushed inside the filter pores which will change the transport parameters (Glaus et al. 2008, Aertsens et al. 2011, Van Laer et al. 2014). As an extreme case (upper limit), fits can be done with the assumption that diffusion parameters in filter and clay are equal (F=C). In Appendix D.2 it is shown that D_e for F=C is always larger than for FF. The lower the ratio of the thickness of the filter and the clay, the less impact the filters will have on the diffusion parameters in the clay. Fitting with these two options (FF and F=C) gives an idea of the uncertainty on the parameters and can be considered as bounding values, but note that this is a different approach than used by PSI-LES (explained in 3.1.10). The minimum and maximum values provided by them are based on 2 bounding values for the filters.

The fitted expressions are solutions of the diffusion equation corresponding to the experimental set-up. The optimal values are obtained by minimizing the χ_2 function. Standard error theory is used to get the values of the errors (1σ) on the optimal values.

2.2 Results and discussion

A visual inspection of the clay plugs did not show any irregularities of the samples. Tab. 2-2 gives an overview of the five samples, including the depth of the sample (also indicated in the sample code) and the dimensions of the samples. Since the thickness of the clay plugs was not homogeneous, an average of the thickness measured at four sides is calculated and used afterwards as value for the modelling. Based on the dimensions and on the wet and dry weight of the clay plug (incl. resin), the moisture content could be determined, which could serve as a proxy for the full porosity. This porosity ranged between 6 and 12% and will be compared with the porosity determined from the HTO diffusion.

Tab. 2-2: Clay plug properties of the five samples provided to SCK CEN: thickness, diameter and calculated porosity based on the moisture content

Determined by drying at 105 °C

Sample code	**Sampling depth** [m]	**Thickness clay plug at 4 sides** [mm]				**Thickness** [mm]	**Diameter** [mm]	**Porosity*** [-]
		1	**2**	**3**	**4**	**Average ± st dev**		
TRU1-1-870.23-DI	870.23	12.32	12.03	11.69	12.96	12.3 ± 0.54	64	0.055 ± 0.002
TRU1-1-882.36-DI	882.36	13.40	14.24	13.92	13.72	13.8 ± 0.35	64	0.116 ± 0.002
TRU1-1-890.39-DI	890.39	12.74	13.15	13.03	12.66	12.9 ± 0.23	64	0.055 ± 0.002
TRU1-1-902.85-DI	902.85	12.45	12.77	12.50	12.26	12.5 ± 0.21	64	0.095 ± 0.002
TRU1-1-938.90-DI	938.90	12.93	13.10	12.73	13.29	13.0 ± 0.24	64	0.089 ± 0.002

* Based on moisture content

The clay plugs were re-saturated with SPW before starting the diffusion experiments. The composition of the pore water chemistry was monitored after each refreshment in order to be sure that the clay was equilibrated with the SPW. Fig. 2-2 shows for each experiment the composition of the pore water. There were no remarkable differences with the pure SPW composition. It can hence be assumed that after 6 weeks of re-saturation (and 5 refreshments) the equilibration was complete.

During the re-saturation period it was noticed that a few set-ups were leaking a bit (interface sample/flange). The leakages could be solved by screwing the bolts tighter at the locations where leakage was observed. As the clay plugs do not have the same thickness over the whole surface (for TRU1-1-870.23-DI the difference was even more than 1 mm, see Tab. 2-2) this could be an explanation for the initial leakage.

In two clay cores there were, however, indications for a preferential pathway. In clay core TRU1-1-870.23-DI there was an immediate breakthrough for HTO and Cl-36. In addition, the flux was equal for both tracers, which is not expected to occur. Further, the changes in the weights of the source and target reservoir confirmed that there was an advective flow between the two compartments. For clay core TRU1-1-890.39-DI the experiment started to deviate after day 21. The indications were less clear than for core TRU1-1-870.23-DI, but the strange course of the

flux, combined with the differences in weights of the source and target reservoir, showed that after day 21 there was a preferential pathway in this experiment as well. It might be that the screwing of the clay plugs to prevent leakage (due to the difference in thickness of the clay plugs) was too strong and caused cracks/fractures. After unloading the cells, the clay plugs were visually inspected, but nothing could be observed. When the diffusion experiments with Na-22 were started, the cores were re-started as well in case the preferential pathway would have disappeared due to sealing of the clay, but it was clear that the preferential pathway was still present. Core TRU1-1-870.23-DI was immediately stopped and hence, there are no diffusion data available for that sample. Core TRU1-1-890.39-DI showed again only deviating results after a while (similarly as for HTO and Cl-36 diffusion). Although the dataset was not showing a steady-state phase of the flux after the breakthrough (transient phase), the data were nevertheless fitted in order to see how much the parameters differ compared to parameters of the fittings of the PSI-LES dataset.

During the experiments with HTO and Cl-36 the peristaltic pump showed failures between day 21 and 31. During these ten days continuously pumping was not feasible. The solutions were only pumped at regular times (few times during the day) for a time interval of 5 – 10 minutes until a new pump arrived. The concentrations in the target reservoir were a bit more fluctuating, but nevertheless the trend of the fluxes was still clearly visible.

Further, it was noticed that the decrease in volume of the source reservoir was larger than expected from the decrease in volume due to sampling (100 or 200 µL/week). In both series of diffusion experiments, the solution volume decreased ±15% at the end of the experiment. In the series with Na-22, the weight of the solutions was monitored weekly and an average weight loss of 0.250 mL/day was observed. This was in line with the total volume loss during the whole period for the series with HTO and Cl-36.

The only plausible explanation was evaporation through the plastic tubing, since the clay was assumed to be fully re-saturated before starting the experiments, the experimental set-ups were completely closed and no further leakages were observed during the experiments. The evaporation was confirmed by the analysis results of the cations and anions as well. The concentrations were on average 16% higher at the end of the experiments, which means that they were up-concentrated due to the evaporation. The HTO concentration was not affected, since it is assumed to evaporate as well but for Cl-36 and Na-22, also an up-concentration was noted. This explains why the concentration in the source reservoir seemed not to decrease for Cl-36, but stayed around the initial activity. In some cases, the activity even increased. For Na-22 there is a decrease, but the observed decrease is assumed to be underestimated due to the counteracting evaporation effect. In former diffusion experiments performed in other gloveboxes or in the atmosphere we have never observed this strong evaporation. We believe that the very dry atmosphere of this glovebox was acting as a strong driving force for evaporation through the particular plastic tubing (Pharmed Ismaprene and Tygon LMT) we used.

The diffusion experiments with HTO and Cl-36 were performed for 60 days. The diffusion experiments with Na-22 lasted 77 days for TRU1-1-882.36-DI and TRU1-1-902.85-DI, while TRU1-1-938.90-DI was sampled up to 98 days. None of the solutions had visible signs of microbial growth (no biofilms or microbial floccules visible in solution or tubing).

Fig. 2-2: Composition of the SPW (concentrations cations & anions, pH) after equilibration with the clay plugs for the 5 cycles of refreshment

Missing datapoints are due to sample loss (by transferring out of the glovebox).

The experimental data of the diffusion experiments are presented in Appendix E together with the experimental fitting results of the two model approaches. Next to the inlet and outlet concentration, which are fitted as a function of time, the outlet flux is shown as well, because this is more continuous as a function of time. The outlet concentration depends on the time between to replacements: a longer time corresponds to a higher outlet concentration. This leads to a strongly varying outlet concentration, providing a limited overall overview. As illustration, for TRU1-1-938.90-DI, also the graphs of an "absolute" fit (see Appendix D.3) of the outlet concentration only, are shown. In all cases, the fitted parameters are the capacity factor ηR and the apparent diffusion coefficient D_a (m^2/s) (in case of F=C this is the D_a of the overall system of clay and filters; in case of FF this is the D_a of the clay). For HTO and Cl-36, the capacity factor equals the accessible porosity η, since the retardation R is assumed to be 1. These parameters are presented in Tab. 2-3 to Tab. 2-5, together with the D_e calculated from the two fitted parameters.

In principle, the FF approach should provide the best estimate for the transport parameters when the uncertainty on the filter parameters is negligible. However, as discussed before this may not be valid. For the interpretation of diffusion experiments typically conducted at SCK CEN, where we use longer clay plugs (lower ratio of filter thickness/plug thickness). we typically follow the two explained approaches ('FF' and 'F=C'). As explained before, the F=C approach should be seen as an upper value.

HTO diffusion

Despite some experimental issues, the datasets are good and provide trustworthy diffusion data. For clay core TRU1-1-890.39-DI, it was decided to use the data of the first 21 days, due to the indications of the preferential pathway after day 21.

All graphs of the inlet concentration show significant scatter (probably due to small sampling volume and evaporation issues). This is one of the reasons why the optimal values are mainly determined by the outlet concentration, when fitting simultaneously inlet and outlet concentration as a function of time. Other reasons for the dominance of the outlet data on the parameter estimation are (i) the larger relative difference between the outlet data and/or (ii) the larger amount of experimental data. Due to the scatter of the experimental inlet data, an excellent fit of these data is not possible, but it is clear that the trend can be fitted in a sufficient way.

Tab. 2-3 presents the overview of the fitted parameters. The individual values of D_a and η only matter at the start of the experiment (around the moment that the outlet concentration sharply rises from zero). Near the end of the experiment only the effective diffusion coefficient plays a role (expression (10) – Appendix D.2) (depending on whether the fit is done by F=C or FF, this is the D_e for the filter and clay system or for the clay only). In all graphs, the initial rise of the outlet concentration is described well by the fits. The optimal values for η are close to one another for the F=C and FF fits. For cores TRU1-1-882.36-DI, TRU1-1-902.85-DI and TRU1-1-938.90-DI, the values are also very close to the porosity based on the water content (Tab. 2-2), especially for the FF fits. Only for sample TRU1-1-890.39-DI, the porosity calculated from the water content is a bit lower. But for this sample only the data until 21 days were used because of an experimental problem, and as such this experiment is prone to a considerable uncertainty.

As explained in Appendix D.2, the effective diffusion coefficient obtained from the F=C fits is expected to be higher than the value for the FF fits (expression (14) – Appendix D.2)). This is indeed the case for all experiments: the experimental and theoretical ratio of D_e (F=C)/D_e (FF) is ~ 1.3 in all cases. For TRU1-1-938.90-DI, also an absolute FF fit of the outlet concentration is added. Despite a slightly higher η than both other fits, this fit describes the experimental data roughly equally well as both other fits.

Tab. 2-3: Summary of the optimal values of the HTO diffusion parameters obtained by (i) assuming the same transport parameter values in the filters and in the clay (F=C) and (ii) fixing the values of the filter transport parameters (FF)[a]

For TRU1-1-938.90-DI, an additional absolute FF fit was performed for the outlet concentration only. The sum of the clay core thickness L_C and the total filter thickness L_f ($L_f = 2 \times 0.2$ cm = 0.4 cm) is the total length L_{tot} (expression (11) in Appendix D.2). The ratio L_f/L_{tot} provides an estimate of the influence of the filters (see Appendix D.2). In case of an F=C fit, D_e and D_a refer to the overall system of clay and filters and for an FF fit they refer to the clay system only. The apparent diffusion coefficient D_a (m^2/s) and the accessible porosity η are the fitted parameters.

Sample	**L_c** [cm]	**L_f/L_{tot}** [-]		**$D_a \times 10^{-11}$** [m^2/s]	**η** [-]	**$D_e \times 10^{-12}$** [m^2/s]	**η (moisture content)** [-]
TRU1-1-882.36-DI	1.382	0.22	F=C FF	10.8 ± 0.4 7.62 ± 0.08	0.110 ± 0.006 0.111 ± 0.005	10.9 ± 0.8 8.64 ± 0.41	0.116 ± 0.002
TRU1-1-890.39-DI[b]	1.290	0.24	F=C FF	10.4 ± 0.6 7.13 ± 0.31	0.110 ± 0.016 0.117 ± 0.015	11.4 ± 1.8 8.34 ± 1.13	0.055 ± 0.002
TRU1-1-902.85-DI	1.250	0.24	F=C FF	10.3 ± 0.4 6.65 ± 0.18	0.083 ± 0.005 0.099 ± 0.006	8.50 ± 0.62 6.56 ± 0.42	0.095 ± 0.002
TRU1-1-938-90-DI	1.301	0.24	F=C FF Abs FF	4.73 ± 0.19 2.98 ± 0.08 2.46 ± 0.14	0.070 ± 0.007 0.084 ± 0.007 0.114 ± 0.007	3.32 ± 0.35 2.51 ± 0.23 2.80 ± 0.24	0.089 ± 0.002

[a] $\eta R_f = 0.4$, $D_{a,f} = 3.5\ 10^{-10}$ m^2/s (Aertsens et al. 2011)

[b] Parameters obtained for dataset until day 21 (parameters full dataset: F=C => D_a 8.55 ± 0.50 × 10^{-11} m^2/s, η 0.185 ± 0.021, D_e 15.8 ± 2.0 × 10^{-12} m^2/s, FF => D_a 5.92 ± 0.25 × 10^{-11} m^2/s, η 0.201 ± 0.020, D_e 11.9 ± 1.3 × 10^{-12} m^2/s)

The errors on D_a and η are the errors on the the fit (1σ). Clearly, they are too small to be representative of the real error. The difference between the optimal values obtained by both ways of fitting, provides a more realistic estimate of the real error. In that case, for the effective diffusion coefficient, both the ratio $D_e/1.3$ (D_e determined by F=C) and D_e (determined by FF) are equivalent estimates of the effective diffusion coefficient in the clay.

Since the temperature in the glovebox varied between 21 and 24°C, it is necessary to discuss the possible temperature effect as well. When assuming an activation energy of 20 kJ/mol[2], the difference in temperature could lead to about 9% variation according to the equation $D_e = A \cdot e^{-Ea/RT}$ with A the so-called pre-exponential factor, R =8.314 J/(K mol) the molar gas constant and E_a the activation energy (kJ/mol). This variation is comparable to the relative error of D_e (by error propagation) ranging between 5 and 16%.

At last, it is observed that the effective and apparent diffusion coefficient are significantly lower in TRU1-1-938.90-DI compared to the three other cores, which indicates that the clayrock at this depth has probably different properties.

[2] Average value based on values from Van Loon et al. (2005): E_a(HTO) = 21.1 ± 1.6, E_a(Na) = 21 ± 3.5, E_a(Cl) = 19.4 ± 1.5 in Opalinus Clay.

Cl-36 diffusion

The diffusion of Cl-36 was studied in parallel with HTO. Tab. 2-4 presents the obtained diffusion parameters of these fits.

Considering the experimental data and fits and summarizing the fitted diffusion parameters, the same general conclusions apply as for HTO. First, there is a significant scatter of the inlet concentration with tracer concentrations higher than the initial concentration (due to up-concentration caused by evaporation and due to large errors resulting from the small sampling volumes). Second, the outlet concentrations are consequently predicted. Third, there is a good correspondence (including the factor of ≈ 1.3) between the effective diffusion coefficients obtained by both ways of fitting (F=C and FF). At last, the correspondence with the optimal parameter values obtained by the third fit option (for the filter, a fixed η and a D_a equal to that in the clay) is good (only the result for TRU1-1-938.90-DI is shown).

Regarding the parameter values, it is clear that the porosity η is significantly smaller than the porosity determined for HTO. This confirms that the anion accessible porosity is lower than the total porosity, as expected due to the anion exclusion effect. The anion accessible porosity of Cl-36 ranges between 26% and 51% of the total porosity.

For the D_e values, it is observed that cores TRU1-1-882.36-DI and TRU1-1-902.85-DI have very comparable D_e values, which was also the case for HTO. Nevertheless, the D_a and η values differ both a factor ±2, but in an opposite way, i.e. D_a higher for TRU1-1-902.85-DI and η higher for TRU1-1-882.36-DI. The D_e for Cl-36 in core TRU1-1-938.90-DI is ± 3 times lower than for cores TRU1-1-882.36-DI and TRU1-1-902.85-DI, which was also observed for HTO. Hence, the ratio of $D_{e,Cl}/D_{e,HTO}$ for these three cores are all around the same value (0.16-0.21). For core TRU1-1-890.39-DI the ratio $D_{e,Cl}/D_{e,HTO}$ is, however, different (0.47). This is in agreement with the ratio Q_{HTO}/Q_{Cl} of the cumulative tracer quantity diffused out of the clay core of both HTO and chloride: $Q_{HTO}/Q_{Cl} \approx 4 - 7$ for TRU1-1-882.36-DI, TRU1-1-902.85-DI and TRU1-1-938.90-DI, but $Q_{HTO}/Q_{Cl} \approx 1.3$ for TRU1-1-890.39-DI. For core TRU1-1-890.39-DI only the first 21 days were used for the fittings and as mentioned before, there were indications for a preferential path and the results are less reliable.

It has to be mentioned as well that in sample core TRU1-1-902.85-DI the slope of the fitting is higher than the actual slope of the first ten data points, since the model includes also the higher values of the flux in the later phase. This means that the obtained parameter results should be interpreted with care. The D_e value is very comparable to sample core TRU1-1-882.36-DI, but the determined D_a and η values are respectively 2 times higher and lower (remember that the initial part is crucial to determine the D_a and η separately). This might be an indication that the D_a is overestimated and the η is underestimated. Since these two cores have comparable parameters for HTO, it is reasonable to assume that the D_e of Cl-36 is reliable. Moreover, this type of migration experiments (through-diffusion) is known to determine D_e accurately (and D_a and nR are predicted less accurately).

Tab. 2-4: Summary of the optimal values for the Cl-36 diffusion parameters obtained by (i) assuming the same transport parameter values in the filters and in the clay (F=C) and (ii) fixing the values of the filter transport parameters[a]

For TRU1-1-938.90-DI, an additional absolute FF fit was performed for the outlet concentration only. The sum of the clay core thickness L_C and the total filter thickness L_f (L_f = 2 × 0.2 cm = 0.4 cm) is the total length L_{tot} (expression (11) in Appendix D.2). In case of an F=C fit D_e and D_a refer to the overall system of clay and filters and for an FF fit they refer to the clay system only. The apparent diffusion coefficient D_a (m^2/s) and the accessible porosity η are the fitted parameters.

Sample	**L_c** [cm]	**L_f/L_{tot}** [-]		**$D_a \times 10^{-11}$** [m^2/s]	**η** [-]	**$D_e \times 10^{-12}$** [m^2/s]
TRU1-1-882.36-DI	1.382	0.22	F=C FF	4.34 ± 0.09 2.74 ± 0.03	0.041 ± 0.002 0.050 ± 0.002	1.76 ± 0.09 1.37 ± 0.06
TRU1-1-890.39-DI[b]	1.290	0.24	F=C FF	10.8 ± 1.4 6.67 ± 0.77	0.047 ± 0.003 0.059 ± 0.014	5.03 ± 1.44 3.96 ± 1.04
TRU1-1-902.85-DI	1.250	0.24	F=C FF	8.93 ± 0.73 5.32 ± 0.39	0.020 ± 0.003 0.026 ± 0.001	1.77 ± 0.26 1.37 ± 0.12
TRU1-1-938-90-DI	1.301	0.24	F=C FF Abs FF	2.37 ± 0.08 1.48 ± 0.02 1.73 ± 0.04	0.029 ± 0.003 0.033 ± 0.003 0.027 ± 0.002	0.68 ± 0.07 0.49 ± 0.04 0.46 ± 0.04

[a] ηR_f = 0.4, $D_{a,f}$ = 3.5 10^{-10} m^2/s (Aertsens et al. 2011)

[b] Parameters obtained for dataset until day 21 (parameters full dataset: F=C => D_a 5.74 ± 0.64 × 10^{-11} m^2/s, η 0.178 ± 0.037, D_e 10.2 ± 2.4 × 10^{-12} m^2/s, FF => D_a 4.09 ± 0.64 × 10^{-11} m^2/s, η 0.176 ± 0.037, D_e 7.20 ± 1.89 × 10^{-12} m^2/s

Na-22 diffusion

After finishing the diffusion experiments with HTO and Cl-36, the diffusion of Na-22 was studied. Tab. 2-5 presents the optimal values of the diffusion parameters determined from the fits.

Both ways of fitting (F=C, FF) describe the experimental data roughly equally well. The relation between the optimal values obtained by F=C and FF is the same as for HTO and Cl and has been explained there. The differences between the different model approaches represent the uncertainty on the parameters.

The D_a values were lower compared to HTO and varied maximum a factor 3 among the different cores. Also, for Na-22, it is clear that core TRU1-1-938.90-DI has lower diffusion parameters compared to the three other cores.

As mentioned before, there were strong indications of a preferential path for core TRU1-1-890.39-DI. Nevertheless, the data have been fitted. The scatter on the outlet flux is high and the outlet flux does not evolve to a steady-state phase, while it does for cores TRU1-1-882.36-DI, TRU1-1-902.85-DI and TRU1-1-938.90-DI. This results in a higher error on D_a than in the three remaining experiments, but also the value of the other parameters of core TRU1-1-890.39-DI should be considered with care. Nevertheless, the values of the parameters do not differ much from cores TRU1-1-882.36-DI and TRU1-1-902.85-DI.

While for HTO and Cl-36 the capacity factor equals the accessible porosity, the higher ηR values indicate that there is a slight sorption of Na-22. The retardation factor of Na-22 is calculated (Tab. 2-6) by dividing the capacity factors of Na and HTO. The retardation factor of Na-22 ranges between 2.5 and 5.8.

Compared to the neutral HTO tracer, it is observed that $D_{a,Na}$ is 3 to 4 times lower than $D_{a,HTO}$, but $D_{e,Na}$ differs less than a factor 2 with $D_{e,HTO}$ or even $D_{e,Na} \approx D_{e,HTO}$ since Na-22 is slightly retarded (R between 2.5 and 5.7, Tab. 2-6).

Tab. 2-5: Summary of the optimal values for the Na-22 diffusion parameters obtained by (i) assuming the same transport parameter values in the filters and in the clay (F=C) and (ii) fixing the values of the filter transport parameters[a]

The sum of the clay core thickness L_C and the total filter thickness L_f ($L_f = 2 \times 0.2$ cm = 0.4 cm) is the total length L_{tot} (expression (11) in Appendix D.2). The apparent diffusion coefficient D_a (m^2/s) and the accessible porosity η are the fitted parameters.

Sample	**L_c** [cm]	**L_f/L_{tot}** [-]		**$D_a \times 10^{-11}$** [m^2/s]	**ηR** [-]	**$D_e \times 10^{-12}$** [m^2/s]
TRU1-1-882.36-DI	1.382	0.22	F=C FF	2.78 ± 0.06 1.81 ± 0.03	0.576 ± 0.046 0.720 ± 0.049	16.0 13.0
TRU1-1-890.39-DI[b]	1.290	0.24	F=C FF	3.95 ± 0.17 2.48 ± 0.06	0.346 ± 0.040 0.436 ± 0.043	13.7 10.8
TRU1-1-902.85-DI	1.250	0.24	F=C FF	2.95 ± 0.05 1.81 ± 0.02	0.306 ± 0.012 0.383 ± 0.013	9.03 6.93
TRU1-1-938-90-DI	1.301	0.24	F=C FF	1.40 ± 0.03 1.06 ± 0.02	0.174 ± 0.010 0.185 ± 0.010	2.44 1.96

[a] Full dataset has been fitted, although there were indications for a preferential path (scatter on outlet flux is high and outlet flux does not evolve to a steady-state phase).

Tab. 2-6: Values of the clay capacity factor for Na-22 and for HTO (from FF fits)

Since HTO is unretarded (R=1) and porosity for HTO and Na-22 are assumed to be equal, the ratio of these capacity factors (ηR) equals the retardation factor R for Na-22.

Sample	**ηR Na-22**	**ηR HTO**	**R Na-22**
TRU1-1-882.36-DI	0.720 ± 0.049	0.111 ± 0.005	6.49 ± 0.54
TRU1-1-890.39-DI[b]	0.436 ± 0.043	0.117 ± 0.015	3.73 ± 0.60
TRU1-1-902.85-DI	0.383 ± 0.013	0.099 ± 0.006	3.87 ± 0.26
TRU1-1-938-90-DI	0.185 ± 0.010	0.084 ± 0.007	2.20 ± 0.23

3 Experiments @PSI-LES

3.1 Materials & methods

3.1.1 Samples and sample preparation

The samples used in the diffusion experiments originate from the Trüllikon-1 bore hole and were selected by staff from the University of Bern (u^b). A list of the samples is given in Tab. 3-1. The samples were prepared at the University of Bern. The preparation steps are summarised in Fig. 3-1. A subsample with a diameter of 64 mm was drilled perpendicular to the bedding plane from a larger core (ca. 100 mm) by dry drilling using a Hilti® drilling machine. The sub-core was embedded in epoxy resin (Epofix, Struers, Germany). After hardening at 40 °C overnight, a slice with a thickness of ca. 12-14 mm was prepared by dry cutting. All manipulations were performed under oxic conditions (air atmosphere). The samples were put in vacuum bags and shipped to PSI-LES.

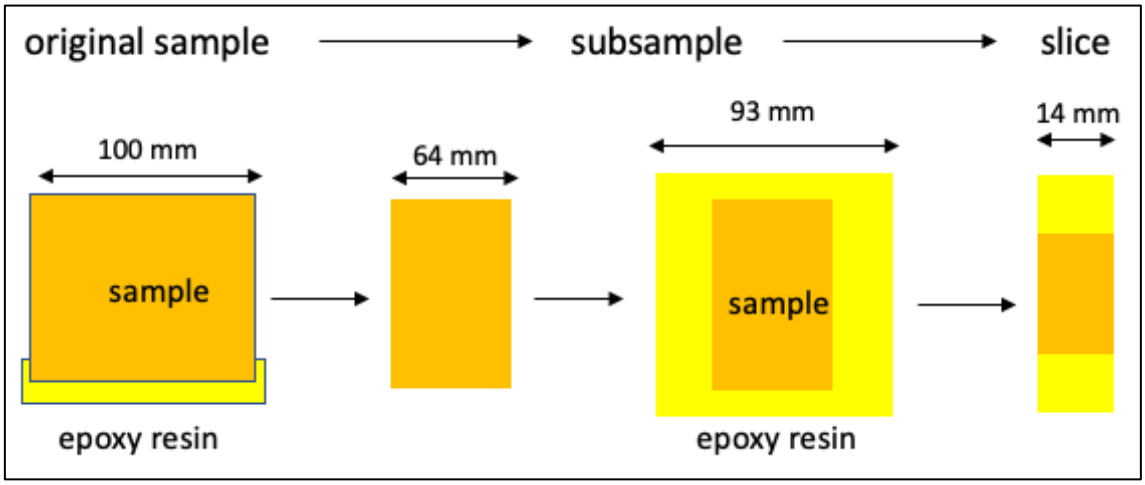

Fig. 3-1: Steps for preparation of clay rock samples for diffusion measurements

The bedding plane is perpendicular to the core axis.

At PSI-LES the samples were unpacked, photographed (Fig. 3-2) and visually inspected for mechanical damages. After polishing the samples using a P420 abrasive paper, the exact dimensions (thickness and diameter) were determined and entered in an Excel spreadsheet. The thickness was measured at 4 points. The average thickness was used for modelling purposes.

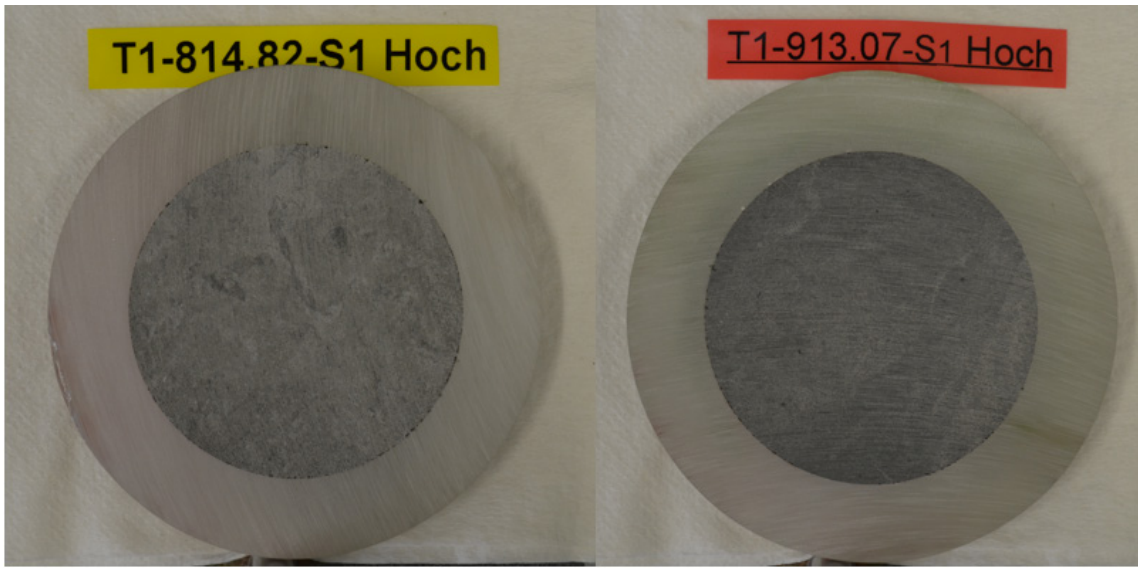

Fig. 3-2: Picture of two sample slices embedded in epoxy resin

3.1.2 Synthetic pore water

SPW was used in all experiments; its composition is given in Tab. 2-1. The SPW is prepared as described in Baeyens (2019).

3.1.3 Diffusion cells

The diffusion cells were made of Ertalyte®, an unreinforced polyester based on polyethylene terephthalate. Porous AISI 316 stainless steel filters (∅ = 65 mm, thickness L = 1.2 mm, pore size 10 μm; porosity 40%) are used to confine the samples. The through-diffusion cell allows to use samples that hardly swell with a diameter of ~65 mm and a thickness between 5 and 20 mm.

3.1.4 Glovebox

All experiments were performed under anoxic conditions in a glovebox (MBraun, Munich, Germany). The glovebox was filled with a mixture of N_2 and CO_2. The CO_2 concentration was 400 ± 10 ppm. The concentration of O_2 in the glove box was < 0.1 ppm.

3.1.5 Diffusion measurements

The clay rock samples were sandwiched between two porous stainless-steel filters and mounted in the diffusion cells with the bedding plane perpendicular to the direction of diffusion. The end plates were fixed by a set of four bolts. The cells were connected to 2 reservoirs (a 100 mL glass flask and a 20 mL polyethylene β-vial), both containing 20 mL synthetic pore water (SPW) that was circulated using a peristaltic pump (IPC, Ismatec, Idex corporation, USA). The solutions were exchanged once per week and analysed for main anions and cations by ion chromatography. As soon as the composition of the pore water was constant (note: as a rule of thumb this is the case after a re-saturation period of ca. 1 month), diffusion measurements were started. To this end the high concentration reservoir (100 mL glass flask) was filled with 100 mL SPW spiked with HTO and $^{36}Cl^-$. The activity in this reservoir was ca. 500 Bq/mL for HTO (ca. 4.5×10^{-10} mol dm^{-3}) and

and $^{36}Cl^-$. The activity in this reservoir was ca. 500 Bq/mL for HTO (ca. 4.5×10^{-10} mol dm^{-3}) and ca. 500 Bq/mL for $^{36}Cl^-$ (ca. 10^{-5} mol dm^{-3}). The low concentration reservoir (20 mL polyethylene β-vial) was filled with 10 mL SPW. The solution at the low concentration side was regularly replaced after a time interval Δt of typical 2 – 3 days to keep the concentration of the tracer in this compartment as low as possible. Diffusion measurements were performed in an inert gas glove box under anoxic conditions (O_2 < 0.1 ppm; CO_2 = 400 ± 10 ppm). The temperature in the glove box was 26.7 ± 0.8 °C.

The experiments with ^{22}Na were started as soon as diffusion of $^{36}Cl^-$ (and HTO) had reached the steady state phase (constant flux). To this end a given amount of $^{22}Na^+$ tracer was added to the source reservoir. The activity of $^{22}Na^+$ was 500 Bq/mL or 200 Bq/mL (ca. 9.5×10^{-11} and 3.8×10^{-11} mol dm^{-3}, respectively). The low concentration side was connected to a 20 mL polyethylene β-vial containing 10 mL SPW. The experimental protocol was identical to that described above for HTO/$^{36}Cl^-$.

3.1.6 Water content measurements

After finishing the diffusion experiments, the diffusion cells were taken apart and the water content (kg) of the samples with thickness L_s (m) and diameter D_s (m) was measured. To this end the samples were dried in an oven at 105 °C until constant weight. The total weight loss W_T (kg) was corrected for weight loss, W_r (kg), caused by heating the resin. The weight loss by the resin was measured by heating a specimen of resin at 105 °C until constant weight. Because the amount of resin was the same for all samples, the weight loss of the resin can be normalised to the sample thickness (0.02g/mm). The water loss porosity (ε_{wl}) was calculated with ρ_w the density of water (998 kg m^{-3} at 20 °C):

$$\varepsilon_{wl} = \frac{4 \cdot (W_T - W_r)}{\rho_w \cdot \pi \cdot L_s \cdot (D_s)^2} \quad (3)$$

3.1.7 Analytics

The ^{22}Na activity in the sampled solutions was measured by γ-counting in a total volume of 5 mL. Five mL of downstream solutions, or 0.5 mL of upstream solutions were put in a counting vial and filled with water to the total volume, where necessary. The activity was measured in a γ-counter (Minaxi-γ, Autogamma 5000 series, Canberra-Packard). HTO and ^{36}Cl were measured with β/β discrimination by liquid scintillation counting (LSC) in a total volume of 10 mL aqueous phase. A detailed description of the β/β discrimination is given in Glaus et al. (2017). To this end, 10 mL of downstream solutions or 0.2 mL of upstream solutions, respectively were added to a counting vial, filled with water to the total volume where necessary, and mixed with 10 mL of Ultimagold and subsequently measured by LSC (Tricarb 2250 CA, Canberra-Packard). The main cations (Na^+, K^+, Ca^{2+}, Mg^{2+}, Sr^{2+}) were monitored by ion chromatography on a DX-600 chromatography system (Thermo Fisher Scientific) using an Ionpac CS12a/CG12a separation and pre-columns and a conductivity detector after in-line suppression of the main eluent ions. Similarly, the main anions were monitored by ion chromatography on a ICS5000$^+$ chromatography system (Thermo Fisher Scientific) using an Ionpac AS16/CG16 separation and pre-column system and a conductivity detector after in-line suppression of the main eluent ions. The total inorganic carbon concentrations were measured using a TOC-LCSH carbon analyser (Shimadzu) by conversion to CO_2 upon acidification of the samples with H_3PO_4 and detection of the purged CO_2 using an infrared detector.

3.1.8 Data processing

Data processing, i.e., calculation of the total diffused mass or activity and/or the diffusive flux, is described in detail in Van Loon & Soler (2003).

3.1.9 Uncertainties

Uncertainty estimations on the values of the flux and total diffused mass are based on the uncertainty propagation of the individual parameter uncertainties involved to calculate these values. The procedure to estimate uncertainties is described in detail in Van Loon & Soler (2003).

3.1.10 Parameter estimation

Modelling of the data is done with Comsol Multiphysics® using the "Transport of Diluted Species in Porous Media" interface involving a 1D-linear geometry for representing the filter and clay domains. The concentration changes in the adjacent upstream solution reservoirs are reflected in variable boundary conditions at the interfaces between filters and solution while a zero-concentration boundary condition was assumed for the downstream side. The variable upstream boundary concentration is calculated from the difference between the total mass present at time zero and the mass diffused from the domain as a function of time. Best-fit parameter values and the respective parameter uncertainties (95% confidence level) are obtained from a parameter optimisation routine (using the lsqnonlin function in Matlab®), in which the Comsol Multiphysics® model is used as a Matlab® script. A short description of the procedure is given in Glaus et al. (2017) and a few additional details are given below.

The total diffused mass at the downstream side and the upstream concentration of the diffusing species as a function of time are used as the source data for parameter fitting. It was shown in a previous measurement campaign for the Bülach-1 borehole, that the use of the downstream flux data instead of accumulated mass leads to similar results. The resulting discrepancies were normally less than the fitting uncertainties. For all three test nuclides, the effective diffusion coefficient in the clay rock and the initial concentration at time zero are treated as adjustable parameters. In the case of HTO, the bulk-dry density (ρ_{bd}) is additionally used as an adjustable parameter. The latter quantity was formally related via a material density (ρ_s) of 2'800 kg m^{-3} to the total porosity (ε) according to the relationship

$$\varepsilon = 1 - \frac{\rho_{bd}}{\rho_s} \quad (4)$$

For this reason, the best-fit parameter value of ρ_{bd} has no physical meaning; it is just used as a fitting parameter because it is available as a primary parameter in the Comsol Multiphysics model, whereas the porosity is not directly addressable therein.

In the case of the $^{36}Cl^-$ data, the anion porosity fraction (f_{an})

$$f_{an} = \frac{e_{an}}{\varepsilon} \quad (5)$$

is used as the third adjustable parameter in combination with the given total porosity for HTO from the parent experiment.

Similarly, R_d is used as the third adjustable parameter in the case of the $^{22}Na^+$ data via the definition of a 1-site Langmuir isotherm in which the affinity constant is chosen in a way to keep the experimental data in a "linear sorption range" (Glaus et al. 2020). Again, the value of the total porosity for the $^{22}Na^+$ data is chosen according to the best-fit parameter value obtained from the HTO data.

Although the initial concentration is an experimentally known value, it is treated as an adjustable parameter (within a rather narrow range of possible values) for cases where there would be a discrepancy between the measured value at time zero and the extrapolation from the subsequent measurements at the following time points. The uncertainties of the diffusion properties of the confining filters on the best-fit parameter values of the adjustable parameters are estimated from a sensitivity analysis because no pertinent values for the diffusivity in the filters were measured and because the contribution of the filter uncertainty to the overall parameter uncertainty cannot be specified universally to all cases (variable effective diffusion coefficients for clay, constant effective diffusion coefficient for filter, see Glaus et al. 2015). Based on experience values from other filters (Glaus et al. 2008) we consider the following bounding values for the filter diffusion coefficients for HTO $5 \times 10^{-11} < D_{e\_fil} < 1.5 \times 10^{-10}$ m^2 s^{-1} (preferred value: 1.0×10^{-10} m^2 s^{-1}) . These upper and lower limits are used for two "bounding" parameter optimisation scenarios (in Matlab), which then produce upper and lower bounds for the adjustable parameter values (with regard to filter uncertainties). The best-fit parameter values for the preferred filter value were calculated as the average of the two bounding "filter scenarios". The maximum and minimum uncertainty values obtained in the two scenarios were used as the upper and lower bounds of the best-fit parameter values. For $^{22}Na^+$, the preferred effective diffusion coefficient for the filters is 6×10^{-11} m^2 s^{-1}, with 3×10^{-11} m^2 s^{-1} and 9×10^{-11} m^2 s^{-1} as the lower and upper, respectively, bounding values. These values are derived from the proportionality of the aqueous bulk diffusion coefficients of the respective tracers and are furthermore consistent with experience values (Aldaba et al. 2014). In the case of $^{36}Cl^-$, a D_{e_fil} value of 1.0×10^{-10} m^2 s^{-1} was used, but no sensitivity analysis was carried out for the filter diffusivities in view of the very low effective diffusivities of this tracer in the clay.

Finally note that the diameter of the confining filters is slightly larger 65 ± 0.5 mm, compared to the diameter of the clay (63.6 ± 0.1) mm. It was demonstrated by a 2-D simulation (not shown) that ignoring the overlapping domains of the filters had no significant influence on the best-fit parameter values and their uncertainties.

3.2 Results and discussion

An overview of the samples with samples thickness (L_s), diameter (D_s) and porosity values ε_{WL} (as derived from the water loss measurements at 105 °C after finishing the diffusion measurements on $^{22}Na^{+}$) are summarized in Tab. 3-1. The visual inspection of the samples showed no abnormalities. So, all samples could be used as received for diffusion measurements. The thickness of the samples as measured on 4 different locations shows a variation of more than 1 mm. The average thickness of the samples (L_s) was used for the calculations.

Tab. 3-1: Clay plug properties of the five samples provided to PSI-LES: thickness, diameter and calculated porosity based on the moisture content (determined by drying at 105 °C)

Sample	**Thickness of the clay plug at 4 points** [mm]				**L_s** [mm] **average ± sigma**	**D_s** [mm]	**ε_{WL}** [-]
	1	**2**	**3**	**4**			
TRU1-1-870.23-DI	12.19	12.35	12.15	12.14	12.21 ± 0.10	63.50	0.092 ± 0.006
TRU1-1-882.36-DI	13.54	13.30	13.16	13.30	13.33 ± 0.16	63.72	0.117 ± 0.008
TRU1-1-890.39-DI	14.10	13.47	12.97	12.91	13.36 ± 0.55	63.50	0.097 ± 0.006
TRU1-1-902.85-DI	14.12	13.50	14.68	13.94	14.06 ± 0.49	63.62	0.102 ± 0.007
TRU1-1-938.90-DI	14.41	14.31	14.89	14.50	14.53 ± 0.25	63.60	0.103 ± 0.007

The evolution of the concentration of major cations and anions, and pH of the SPW during the re-saturation phase is given in Fig. 3-3 to Fig. 3-7. The starting composition of the SPW is marked as "SPW". In total four replacements of SPW with an interval of 1 week were performed. No major changes in the composition of the pore water can be observed indicating that the SPW is in equilibrium with the clay sample.

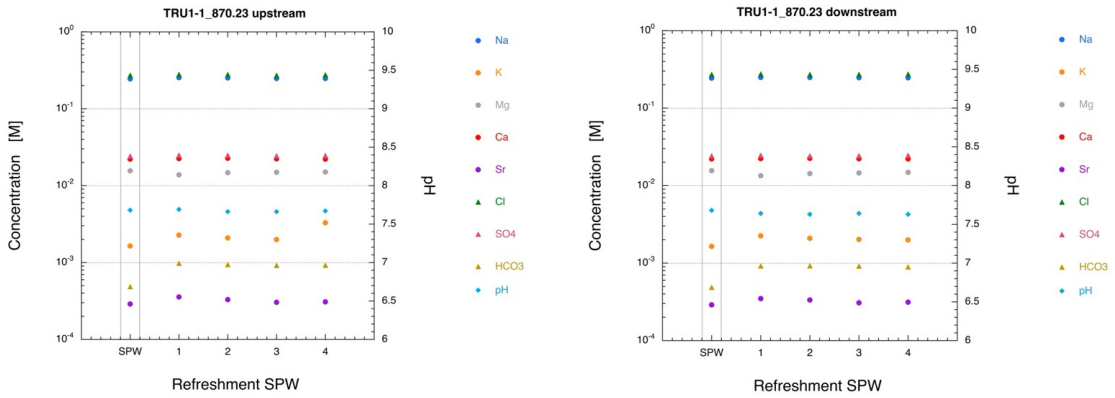

Fig. 3-3: Evolution of the concentration of major cations and anions, and pH in SPW in contact with sample TRU1-1-870.23-DI

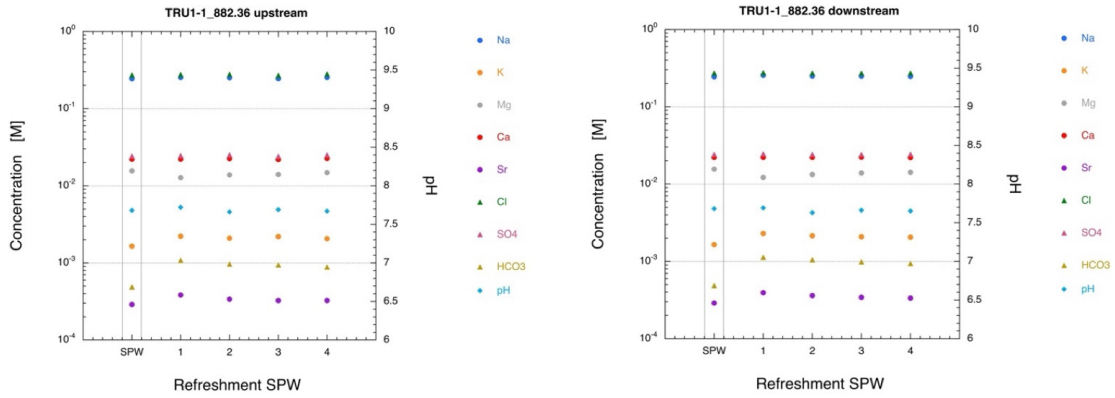

Fig. 3-4: Evolution of the concentration of major cations and anions, and pH in SPW in contact with sample TRU1-1-882.36-DI

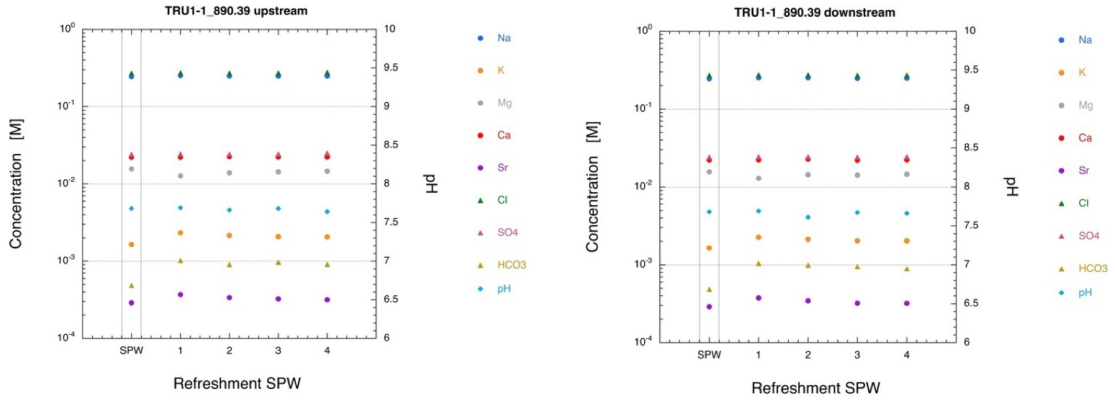

Fig. 3-5: Evolution of the concentration of major cations and anions, and pH in SPW in contact with sample TRU1-1-890.35-DI

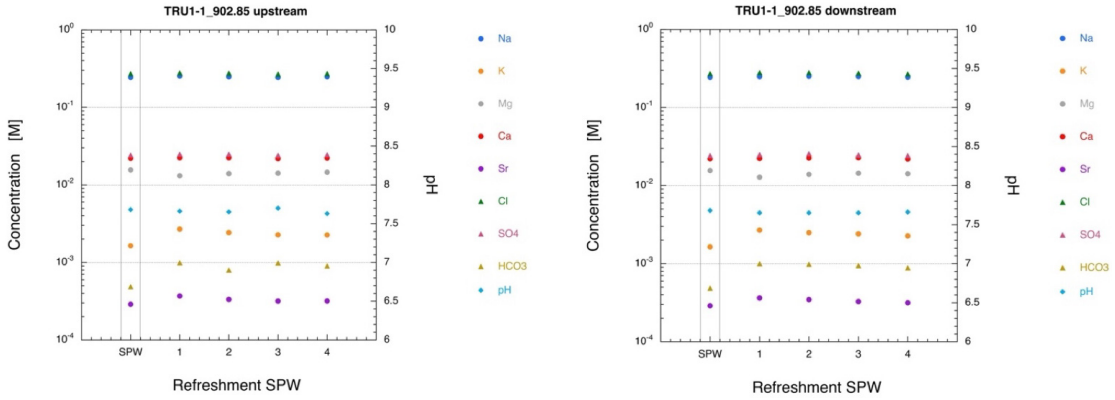

Fig. 3-6: Evolution of the concentration of major cations and anions, and pH in SPW in contact with sample TRU1-1-902.85-DI

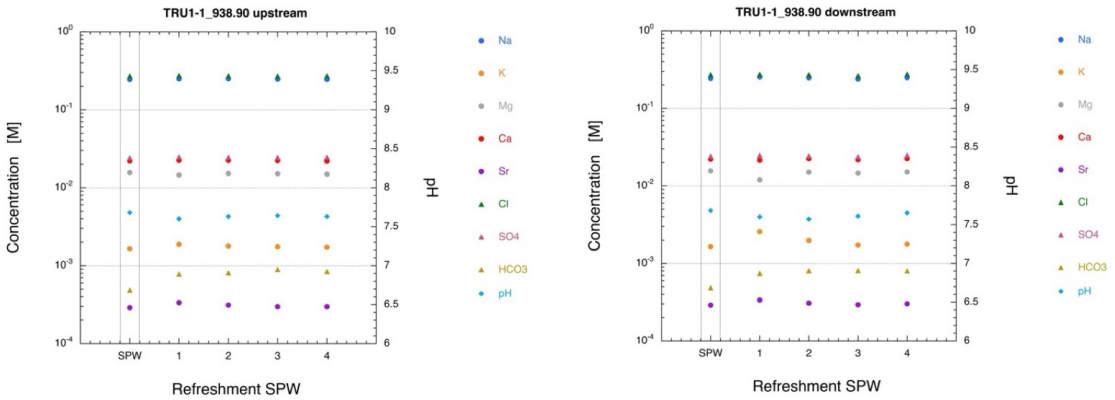

Fig. 3-7: Evolution of the concentration of major cations and anions, and pH in SPW in contact with sample TRU1-1-938.90-DI

An overview of the results for the different elements is given in Tab. 3-2 to Tab. 3-4. In the case of $^{22}Na^{+}$, the accessible porosity (ε_{acc}) [3] of HTO was used in the calculations and the R_d value was optimised.

Tab. 3-2: Results of the parameter optimization of the diffusion experiments with HTO

Sample	D_e (m^2/s)	ε_{acc} (-)
TRU1-1-870.23-DI	$(7.64 \pm 0.24) \times 10^{-12}$	0.121 ± 0.007
TRU1-1-882.36-DI	$(1.23 \pm 0.05) \times 10^{-11}$	0.134 ± 0.009
TRU1-1-890.39-DI	$(9.44 \pm 0.31) \times 10^{-12}$	0.129 ± 0.008
TRU1-1-902.85-DI	$(8.07 \pm 0.26) \times 10^{-12}$	0.134 ± 0.007
TRU1-1-938.90-DI	$(2.95 \pm 0.21) \times 10^{-12}$	0.092 ± 0.009

Tab. 3-3: Results of the parameter optimization of the diffusion experiments with $^{36}Cl^{-}$

Sample	D_e (m^2/s)	ε_{acc} (-)
TRU1-1-870.23-DI	$(2.54 \pm 0.07) \times 10^{-12}$	0.053 ± 0.003
TRU1-1-882.36-DI	$(2.37 \pm 0.10) \times 10^{-12}$	0.060 ± 0.004
TRU1-1-890.39-DI	$(1.98 \pm 0.07) \times 10^{-12}$	0.058 ± 0.003
TRU1-1-902.85-DI	$(1.53 \pm 0.04) \times 10^{-12}$	0.058 ± 0.002
TRU1-1-938.90-DI	$(4.93 \pm 0.70) \times 10^{-13}$	0.035 ± 0.008

[3] Note that different symbols are used for the accessible porosities by SCK CEN (η) and PSI-LES (ε_{acc}).

Tab. 3-4: Results of the parameter optimization of the diffusion experiments with $^{22}Na^{+}$

Sample	D_e (m^2/s)	R_d (m^3/kg)
TRU1-1-870.23-DI	$(9.47 \pm 0.37) \times 10^{-12}$	$(1.16 \pm 0.09) \times 10^{-4}$
TRU1-1-882.36-DI	$(1.65 \pm 0.09) \times 10^{-11}$	$(1.27 \pm 0.07) \times 10^{-4}$
TRU1-1-890.39-DI	$(1.16 \pm 0.05) \times 10^{-11}$	$(1.21 \pm 0.10) \times 10^{-4}$
TRU1-1-902.85-DI	$(1.05 \pm 0.04) \times 10^{-11}$	$(1.34 \pm 0.08) \times 10^{-4}$
TRU1-1-938.90-DI	$(2.63 \pm 0.07) \times 10^{-12}$	$(7.40 \pm 0.54) \times 10^{-5}$

4 Benchmark study

In this part the parameters obtained independently by both institutes are compared to each other. In addition, there was a limited benchmark modelling exercise performed for the HTO and Cl-36 diffusion experiments as well. The experimental datasets were exchanged and parameters were determined with the models of each institute.

Fig. 4-1 shows the diffusion parameters obtained independently for each core. For the PSI-LES dataset, the bounding values of the best-fit parameter values are given, while for SCK CEN the best-fit parameter values of the two model approaches (FF and F=C) are given. These scenarios are seen as representative for the fitting uncertainties. The FF approach of SCK CEN is a similar approach as the PSI approach, with fixed parameters for the filter diffusion coefficient and capacity factor. The filter D_e value used at SCK (for all tracers) almost equals the maximum D_e for the filter used by PSI-LES. In this respect the SCK CEN FF parameters can be best compared to the PSI min value.

When comparing the values of both institutes, it has to be kept in mind as well that the clay cores – although samples taken next to each other – might have slightly different structural and diffusion properties due to sample heterogeneity. This can be seen in the data of water loss data (Tab. 2-3 and 3-1) measured after the diffusion experiments by drying the clay rock samples. Although the same experimental steps were applied in this procedure including the same correction for weight loss of the resin, discrepancies larger than the experimental uncertainties remain. No obvious explanation in terms of experimental procedures is available to explain these discrepancies. Furthermore, there is an effect of temperature. The experiments at PSI-LES have been done at higher temperature which will lead to higher diffusion coefficients (~ 12%, see later).

The most important difference between the modelling approaches of PSI-LES and SCK CEN is the way that the parameters are fitted. The SCK CEN approach consists of optimising the D_a and ηR values and then D_e is calculated by multiplying D_a and ηR. PSI-LES optimises the D_e value instead of D_a and uses a different approach for ηR for the different tracers. In case of HTO and Cl-36 the accessible porosity η [4] ($=\eta R$, because $R=1$) is optimized as well, but for the sorbing Na-22 tracer the R_d (sorption distribution coefficient) is the fitting parameter. The R_d can be converted to R by the equation $R = 1 + (\rho_b/\eta)\, R_d$ with η the porosity determined from the diffusion of HTO and ρ_b the bulk density (calculated from the HTO data).

For HTO, the minimum and maximum values obtained for D_e by PSI-LES are situated in between the values obtained by SCK CEN with the two different model approaches for core samples TRU1-1-890.39-DI, TRU1-1-902.85-DI and TRU1-1-938.90-DI. Only for core sample TRU1-1-882.36-DI the PSI-LES values are higher than the SCK CEN values. When comparing the η values, it is clear that the porosity obtained by PSI-LES is higher than the porosity obtained for SCK CEN, although they do not differ too much. For core sample TRU1-1-902.85-DI, the difference is larger than for the other cores, although the D_e values obtained for this core agreed very well. This means that the D_a values differ as well, but then in the opposite way.

For Cl-36, the D_e values of core samples TRU1-1-902.85-DI and TRU1-1-938.90-DI are very comparable and for core sample TRU1-1-882.36-DI the difference is still less than a factor 2. For the reduced dataset of core sample TRU1-1-890.39-DI the obtained parameters by SCK CEN for D_e are a factor 2 to 2.5 higher. The unexpected course of the outlet flux and less good fitting (fitted slope of the transient phase is higher than the slope of the data points) make us conclude that the

[4] Denoted ε_{acc} by PSI-LES

D_e values obtained by SCK CEN for this core sample are overestimated. For the porosity of these core samples, the values agree very well with each other, except for core 902.85-DI where the porosity of SCK is 2 – 3 times lower than the values obtained by PSI-LES. Most plausible is that the fit of the Cl-36 flux in this core (Fig. E-3) is not approaching sufficiently the experimental data in the transient phase (which determines the nR), i.e. the slope of the fit is higher than the slope of the experimental data, which could lead to an underestimation of the parameter.

For Na-22, the D_e values obtained by both institutes are again very comparable. The capacity factor (ηR) was not compared in this case, since the model approach of PSI-LES fits the R_d instead of ηR. Although the R_d could be converted to R, whereby the best-fit parameter values of porosity and bulk density from the HTO experiments are used, we limit the comparison to the D_e values, since assumptions need to be done for the conversion.

For the (limited) benchmark modelling exercise the values obtained by the different model approaches for a specific dataset are compared. Fig. 4-2 shows the values of the diffusion parameters for core sample TRU1-1-882.36-DI obtained by the different model approaches for both experimental datasets. For the PSI-LES model approach, only the average value is given. For the dataset of SCK CEN, both model approaches (F=C and FF) are given, since it is not valid to make an average of these values. For the PSI-LES dataset, only the F=C approach was used by SCK, since the filter parameters were unknown by that moment. Ideally for a dedicated benchmark modelling exercise, similar diffusion parameter values should have been used. This would have allowed to draw a clear conclusion regarding the uncertainties created by the different computational methods, but a modelling benchmark was not the objectives of the project. It is clear that the variability between the model approaches is very similar to the variability between the parameters obtained from the two independent studies. For the other cores (see Appendix G for values in Tab. G-1), the results are very comparable.

At last, also the comparison between the two datasets modelled with the same model approach could be done. Also here, a similar variability can be observed. The variability in this case can be due to the small differences in experimental approach, but can also be attributed to possible sample heterogeneity. Although the two samples were replicates taken next to each other in the drilling core, we have to take into account that there can still be sample heterogeneity which can cause differences in diffusion properties.

The benchmark study shows that diffusion experiments conducted by different labs on samples of same origin using the same basic experimental approach but using their own ways of data reduction provide comparable parameters with comparable uncertainty ranges but some differences are observed. The differences obtained in parameters by both labs can be explained by different reasons, all discussed below. Tab. 4-1 gives in addition the deviations between the minimum and maximum values obtained by both institutes and the deviation between both institutes.

The fit error on the parameter indicates how well the data are fitted by the parameter. The errors for the D_e values of SCK CEN (propagated from the fit errors on D_a and ηR) are typically below 10%. With a poor fit of the data, an increase up to 25% can occur. This is especially attributed to the error on ηR. Experimental errors have as a consequence that the concentration or flux profile can be interpreted less good. Individual analysis errors can be ignored, since the fit is based on the total profile. In case of experimental problems (leading to scattered or doubtful data), the timing of when the problems occur determines which parameter is mostly affected. Problems occurring at the start or during the transient phase will have their effect on the individual values of D_a and ηR, while problems in the steady-state phase will affect the D_e (= D_a ηR).

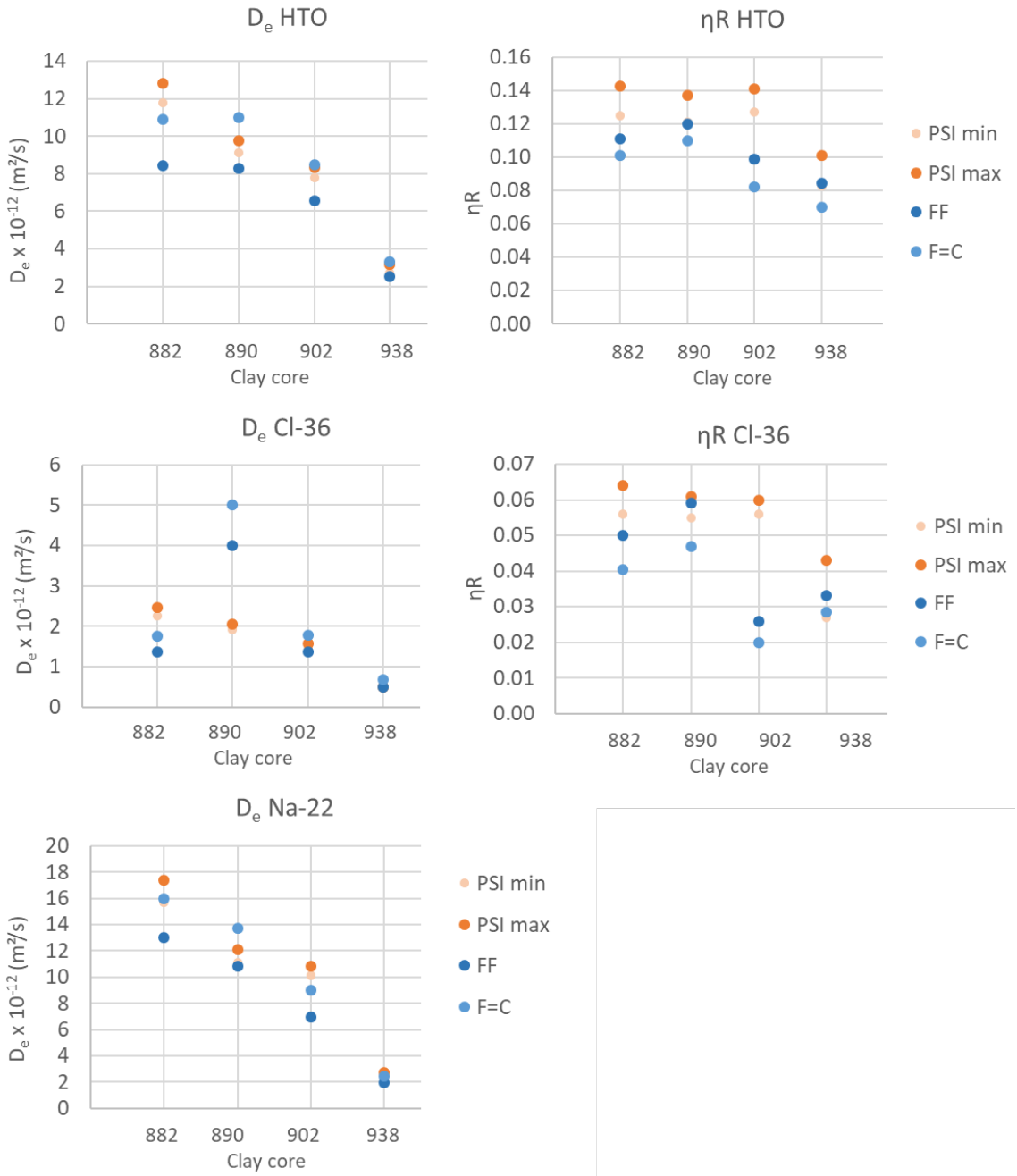

Fig. 4-1: Diffusion parameters of HTO, Cl-36 and Na-22 obtained for the four cores (TRU1-1-882.36-DI, TRU1-1-890.39-DI, TRU1-1-902.85-DI and TRU1-1-938.90-DI) by SCK CEN (approaches FF and F=C) and by PSI-LES (min and max values)

For Na-22 only D_e is given, since PSI-LES and SCK CEN fit different parameters (R_d vs ηR).

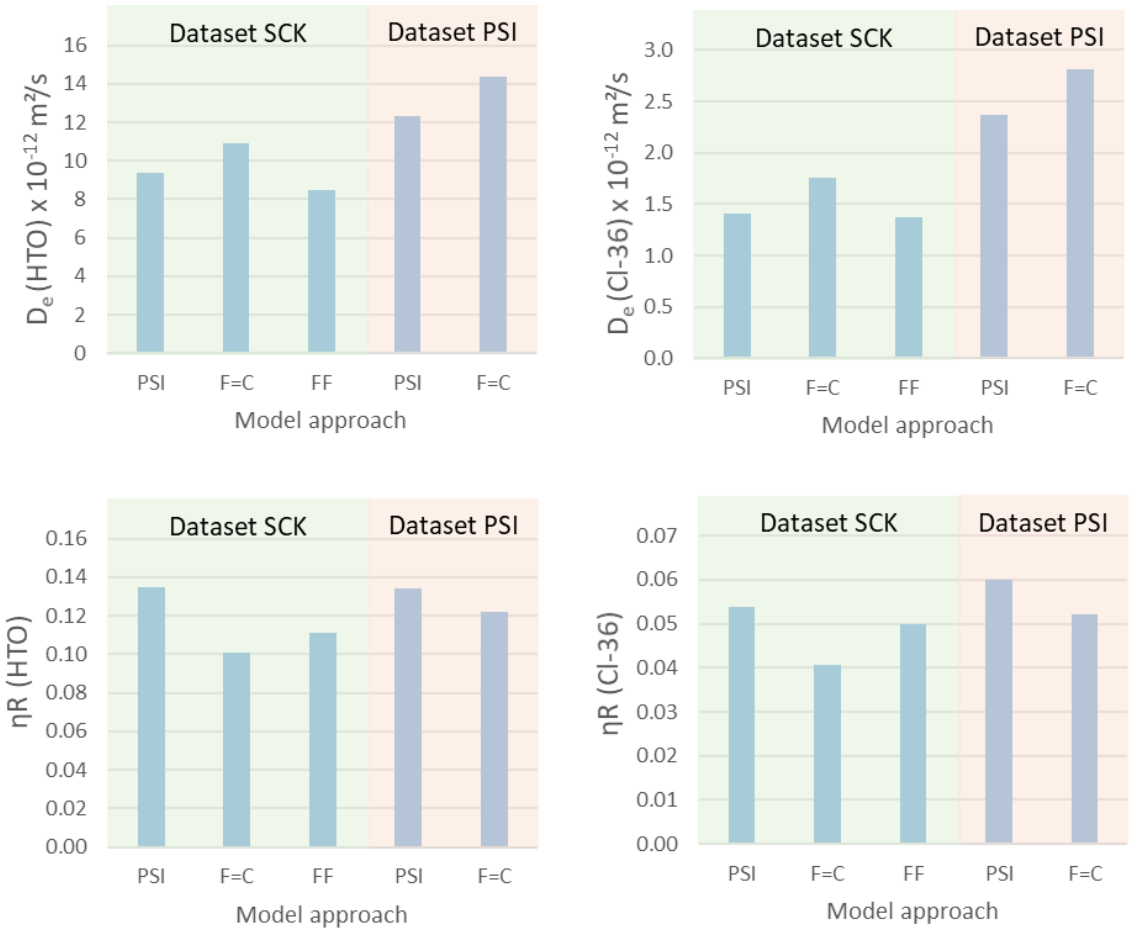

Fig. 4-2: Diffusion parameters of HTO and Cl-36 obtained with the different model approaches for the datasets of SCK CEN and PSI-LES for core sample TRU1-1-882.36-DI

There is the temperature difference that will cause differences, since the experiments at PSI-LES were performed at a slightly higher temperature (26.7 °C) than at SCK CEN (T varied between 21 and 24 °C). According to equation $D_e = A \cdot e^{-Ea/RT}$ (with A the so-called pre-exponential factor, R =8.314 J/(K mol) the molar gas constant and E_a the activation energy (kJ/mol)), the diffusion coefficient D_e of HTO at (PSI-LES) will be about 8 – 17% higher than the diffusion coefficient determined at SCK CEN (assuming an activation energy of 20 kJ/mol) (Van Loon et al. 2005)). This variation is in the same range as the error on the effective diffusion coefficient. When comparing the values of the 'SCK FF' approach and the 'PSI min' approach (with max filter D_e) (most comparable, since a comparable D_e value for the filter is used), the 'PSI min' value for D_e is indeed always higher than the value determined with the 'SCK FF' approach. For TRU1-1-890.39-DI and TRU1-1-938.90-DI, the difference equals almost the difference estimated due to the temperature effect (about 8 – 17%), but for TRU1-1-882.36-DI and TRU1-1-902.85-DI the difference is higher (resp. 27 and 51%).

Also, the different approach of the incorporation of the filters in the model will lead to small differences in the parameter values. While PSI-LES uses a limited range for the filter diffusion coefficient (factor 3 between min and max value), SCK CEN compares the FF approach (with a fixed value for the filter diffusion coefficient) with the F=C approach, where the filter is assumed to have a similar diffusion coefficient as the clay, which is typically one order of magnitude lower.

Hence, it is logic that the values of the two SCK CEN approaches will vary more than those of PSI-LES (relative deviation 29% vs. 8% – Tab. 4-1). Besides, there is the difference in filter thickness. The filters used by PSI-LES have a thickness of 1.2 mm (L_f/L_{tot} ~ 0.15), while the filters of SCK CEN are 2 mm thick ((L_f/L_{tot} ~ 0.23). As explained in Appendix D.2, the filter thickness has an influence on the diffusion parameters and the impact is higher when the L_f/L_{tot} increases.

It is expected that the different way of fitting the parameters (D_a and ηR at SCK CEN vs. D_e and ηR at PSI-LES) will have an effect as well on the parameters, especially on the ηR (for D_e the impact is less). This is confirmed by the results of the benchmark modelling exercise (Fig. 4-2), where is shown that the difference between the D_e values determined by PSI-LES (on SCK CEN data) and SCK CEN (FF approach) is quite small while this is more apparent for ηR values.

The best comparison can be made between the FF approach of SCK CEN and the fitting of PSI-LES with the maximum D_e for the filter (corresponding to the D_e min value for HTO and Cl-36)[5]. Without correction for the temperature, the deviation for the different radionuclides and experiments is on average 26% (ranging between 3 and 70%). When performing a temperature correction of 10%, the difference becomes less with an average of 19% and values varying between 1 and 56%.

When considering the obtained upper and lower values over the two labs, we observe deviations between 8 and 77%, which include the most important effects that will influence the data (experimental data, temperature, filter, modelling approach).

To conclude, when different labs perform diffusion experiments on clay samples originating from the same clay core with a similar experimental approach but in an independent way, one should take into account that the obtained parameters could differ within a factor 2 (100%). Optimisation can lower this by 20 – 30%.

[5] Note that for Na-22, the maximum D_e value of the filter used by PSI-LES was lower ($9.0\ 10^{-11}$ m²/s) than the value used by SCK CEN ($1.4\ 10^{-10}$ m²/s).

Tab. 4-1: Comparison of diffusion coefficients (min and max values) determined by SCK CEN and PSI-LES with deviations (%) between min and max values and between the FF approach of SCK CEN and PSI (min D_e) values (best combination to compare) for the actual values and for the T corrected value of PSI (10%)

		Parameters SCK						**Parameters PSI**			**SCK vs PSI**		
		F=C Max. D_a	FF Min. D_a	Deviation [%]	F=C Max. D_e	FF Min. D_e	Deviation [%]	Max. D_e	Min. D_e	Deviation [%]	Deviation [%]	Min. D_e	Deviation [%]
		$\times 10^{-11}$ [m^2/s]			$\times 10^{-12}$ [m^2/s]			$\times 10^{-12}$ [m^2/s]				$\times 10^{-12}$ [m^2/s]	
870	HTO Cl Na							7.9 1.57 9.86	7.41 1.51 9.12	7 4 8			
882	HTO Cl Na	10.8 4.34 2.78	7.62 2.74 1.81	42 58 54	10.9 1.76 16	8.64 1.37 13	26 28 23	12.8 2.42 17.4	11.8 2.31 15.7	8 5 11	37 69 21	10.60 2.08 14.10	23 52 9
890	HTO Cl Na	10.4 10.8 3.95	7.13 6.67 2.48	46 62 59	11.4 5.03 13.7	8.34 3.96 10.8	37 27 27	9.77 2.01 12.1	9:16 1.95 11.1	7 3 9	10 51 3	8.24 1.76 9.99	1 56 8
902	HTO Cl Na	10.3 8.93 2.95	6.65 5.32 1.81	55 68 63	8.5 1.77 9.03	6.56 1.37 6.93	30 29 30	8.35 1.55 10.8	7.83 1.51 10.1	7 3 7	19 10 46	7.05 1.36 9.09	7 1 31
938	HTO Cl Na	4.73 2.37 1.4	2.98 1.48 1.06	59 60 32	3.32 0.68 2.44	2.51 0.49 1.96	32 39 24	3.16 0.53 2.7	2.75 0.458 2.57	15 16 5	10 7 31	2.48 0.412 2.31	1 16 18

5 Conclusion

This study consisted of performing through-diffusion experiments of three tracers, HTO, Cl-36 and Na-22, resp. a neutral anionic and a cationic species, on five "duplicate" samples (samples taken next to each other) of clay material from the Trüllikon-1 borehole by SCK CEN and PSI-LES. Unfortunately, the through-diffusion results in clay core sample TRU1-1-870.23-DI at SCK CEN needed to be abandoned due to indications of a preferential pathway, but the results of the other four cores were sufficient to draw conclusions about the benchmark. The experimental design of both institutes was very comparable, except from some details like the thickness of the filter.

The benchmark study shows an acceptable agreement between the independently performed diffusion studies at both institutes. The variability between the effective diffusion coefficient for each of the three studied radionuclides was less than a factor 2, and often even much lower. Also, the parameter estimations of the capacity factor ηR (which equals the porosity η) for HTO and Cl-36 agreed well between the two institutes. The discrepancies can be ascribed to differences in the experimental approach/conditions(influence of filter thickness, difference in temperature) or the model approach (chosen filter parameters, fitting optimisation strategy), but also possible heterogeneity of the samples cannot be ruled out, even if the duplicate samples are taken next to each other. The good agreement of the parameter values obtained for the majority of the experiments make us conclude that the tests done by different laboratories for (nearly) the same sample material provide consistent results within the expected robustness of the experimental and computational methods.

6 References

Aertsens M., Govaerts J., Maes N. & Van Laer L. (2011): Consistency of the strontium transport parameters in Boom Clay obtained from different types of migration experiments: accounting for the filter plates. Mat. Res. Soc. Symp. Proc.1475, 583-588.

Aertsens, M., Van Laer, L., Maes, N. & Govaerts, J. (2017): An improved model for through-diffusion experiments: application to strontium and tritiated water (HTO) diffusion in Boom Clay and compacted illite. Radioactive waste confinement: Clays in natural and engineered barriers (Eds. S. Norris, J. Bruno, M. Van Geet, E. Verhoef). Geological society, London, Special publications, 443, 205-210.

Aldaba, D., Glaus, M.A., Leupin, O., Van Loon, L.R., Vidal, M. & Rigol, A. (2014): Suitability of various materials for porous filters in diffusion experiments. Radiochimica Acta 102, 723-730.

Baeyens, B. (2019): Herstellung eines synthethischen Porenwassers (SPW) für die Sorptions- und Diffusionsversuche. Arbeitsanweisung AA-LES-12, Paul Scherrer Institut, Villigen PSI, Switzerland.

Glaus, M.A., Aertsens, M., Maes, N., Van Laer, L. & Van Loon, L.R. (2015): Treatment of boundary conditions in through-diffusion: A case study of 85Sr2+ diffusion in compacted illite. Journal of Contaminant Hydrology, 177-178, 239-248.

Glaus, M.A., Frick, S. & Van Loon, L.R. (2017): Diffusion of selected cations and anions in compacted montmorillonite and bentonite. PSI Bericht 17-08, Paul Scherrer Institute, Villigen und Würenlingen, Switzerland. Also published as Nagra Technical Report NTB 17-12.

Glaus, M.A., Frick, S. & Van Loon, L.R. (2020): A coherent approach for cation surface diffusion in clay minerals and cation sorption models: Diffusion of Cs+ and Eu3+ in compacted illite as case examples. Geochim. Cosmochim. Acta 274, 79-96.

Glaus, M.A., Rossé R., Van Loon, L. & Yaroshchuk, A. (2008): Tracer diffusion in sintered stainless steel filers: measurement of effective diffusion coefficients and implications for diffusion studies with compacted clays. Clays and Clay minerals 56, 677-685.

Van Laer, L., Bruggeman, C., Maes, N. & Aertsens, M. (2014): Diffusion of sorbing tracers in compacted clay, EC 7FP Catclay Project Deliverable 2-3. www.catclay.org.

Van Loon, L., Leupin, O. & Cloet, V. (2018): The diffusion of $SO42^-$ in Opalinus Clay: Measurements of effective diffusion coefficients and evaluation of their importance in view of microbial mediated reactions in the near field of radioactive waste repositories. Applied Geochemistry, 98, 19-24.

Van Loon, L., Müller, W. & Iijima, K. (2005): Activation energies of the self-diffusion of HTO, Na-22(+) and Cl-36(-) in highly compacted argillaceous rock (Opalinus Clay). Applied Geochemistry 20, 961-972.

Van Loon, L.R. & Soler, J.M. (2003): Diffusion of HTO, 36Cl–, 125I– and 22Na+ in Opalinus Clay: Effect of confining pressure, sample orientation, sample depth and temperature. PSI Bericht 04-03, Paul Scherrer Institute, Villigen, Switzerland. Also published as Nagra Technical Report NTB 03-07.

Appendix A: Synthetic pore water

Protocol Synthetic pore water (TRU1) (provided by PSI)

Goal: Preparation of 1 or 2 L SPW (AA-LES-12) at pH 7.68 in the glove box (0.04% CO_2 – no O_2)

Chemicals

NaCl, for Analysis, MW = 58.44 g/mol

Na_2SO_4, for Analysis, MW = 142.04 g/mol

$NaHCO_3$, for Analysis, MW = 84.01 g/mol

KCl, for Analysis, MW = 74.55 g/mol

$MgCl_2.6H_2O$,, for Analysis p.a., MW = 203.3 g/mol

$CaCl_2.2H_2O$, for Analysis p.a., MW = 147.01 g/mol

$SrCl_2.6H_2O$, for Analysis p.a., MW = 266.62 g/mol

* Weigh all chemicals precisely and enter them in the glovebox in separate small vials (glass LSC vials). Leave the vials at least 30 min open so that the salts can acclimatise.

Salts	g for 1L	g for 2L
NaCl	11.3796	22.7592
KCl	0.1221	0.2442
Na_2SO_4	3.4535	6.9070
$NaHCO_3$	0.0410	0.0819
$MgCl_2.6H_2O$	3.1636	6.3272
$CaCl_2.2H_2O$	3.2564	6.5128
$SrCl_2.6H_2O$	0.0772	0.1543

* Prepare 1 or 2 L degassed Milli-Q-Water and bring it in the glovebox. Leave the bottle open for 3 days.

Preparing the solution

Fill a flask of 1 or 2 L with ca. 0.7 or 1.5 L degassed MQ water. Dissolve first the alkali salts (Na, K) while continuously stirring. Thereafter the earth alkali salts (Mg, Ca, Sr) are added slowly to the solution. *When mixing more than 1 g the salt should be added stepwise and there should be always waited until everything is dissolved*. Watch if the solution keeps stable. The solution should not become turbid. At last, fill the flask almost to the mark.

Leave the solution over night or over the weekend (without a stopper).

Measure pH. When pH is between 7.6 and 7.8, it should not be adjusted. If not, then it should be adjusted with HCl/NaOH.

After adjusting the pH the magnetic stirrer should be removed and the flask should be filled with MQ water until the mark.

Analytics

Subsamples will be taken for ICP analysis (Na, K, Ca, Mg) (dilution 50x + acidifying with 2% HNO_3), IC analysis (Cl and SO_4) (300x dilution) and TIC analysis (2 mL diluted 10 times to 20 mL).

Appendix B: Design diffusion cell (SCK CEN)

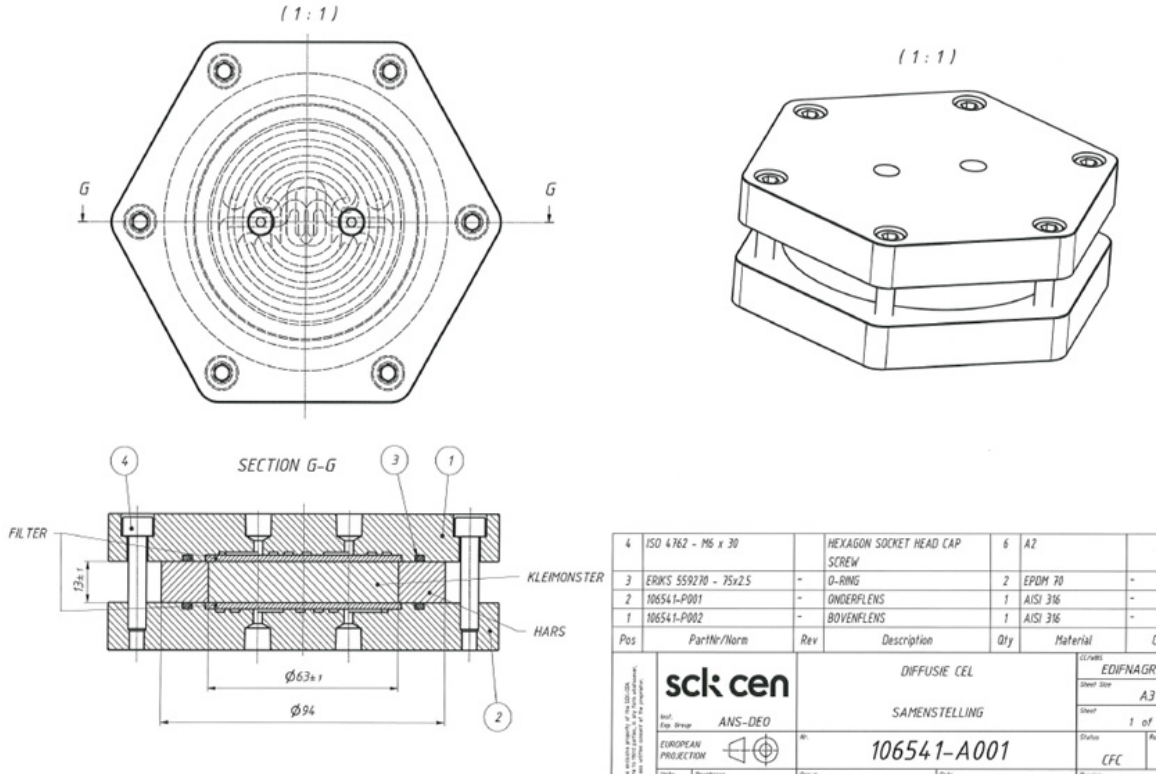

Fig. B-1: Technical drawing of the diffusion cell

Appendix C: Validation/optimisation of radiochemical analysis (SCK CEN)

C.1 Method development and validation of the determination of HTO and Cl-36 activities by means of LSC

Explanation symbols

D_{SH}:	Activity (in dpm) of a high energy nuclide (Cl-36) standard
D_{SL}:	Activity (in dpm) of a low energy nuclide (H-3) standard
D_H:	Activity (in dpm) of high energy nuclide (Cl-36) in the sample
D_L:	Activity (in dpm) of low energy nuclide (H-3) in the sample
A_g:	Total gross count rate (in cpm) of the sample in Region A
B_g:	Total gross count rate (in cpm) of the sample in Region B
$A_g(H)$:	Gross count rate (in cpm) of the high energy nuclide standard in Region A
$B_g(H)$:	Gross count rate (in cpm) of the high energy nuclide standard in Region B
$A_g(L)$:	Gross count rate (in cpm) of the low energy nuclide standard in Region A
$B_g(L)$:	Gross count rate (in cpm) of the low energy nuclide standard in Region B
A_0:	Count rate (in cpm) of the blank in Region A
B_0:	Count rate (in cpm) of the blank in Region B
t_{A_g}:	Measurement time (in minutes) of A_g
t_{B_g}:	Measurement time (in minutes) of B_g
$t_{A_g(H)}$:	Measurement time (in minutes) of $A_g(H)$
$t_{B_g(H)}$:	Measurement time (in minutes) of $B_g(H)$
$t_{A_g(L)}$:	Measurement time (in minutes) of $A_g(L)$
$t_{B_g(L)}$:	Measurement time (in minutes) of $B_g(L)$
t_{A_0}:	Measurement time (in minutes) of A_0
t_{B_0}:	Measurement time (in minutes) of B_0
$A = A_g - A_0$:	Total blank corrected count rate (in cpm) of the sample in Region A
$B = B_g - B_0$:	Total blank corrected count rate (in cpm) of the sample in Region B
$A_H = A_g(H) - A_0$:	Blank corrected count rate (in cpm) of the high energy nuclide standard in Region A
$B_H = B_g(H) - B_0$:	Blank corrected count rate (in cpm) of the high energy nuclide standard in Region B

$A_L = A_g(L) - A_0$: Blank corrected count rate (in cpm) of the low energy nuclide standard in Region A

$B_L = B_g(L) - B_0$: Blank corrected count rate (in cpm) of the low energy nuclide standard in Region B

$E_{HA} = \frac{A_H}{D_{SH}}$: Efficiency of high energy nuclide in Region A

$E_{HB} = \frac{B_H}{D_{SH}}$: Efficiency of high energy nuclide in Region B

$E_{LA} = \frac{A_L}{D_{SL}}$: Efficiency of low energy nuclide in Region A

Defining region settings

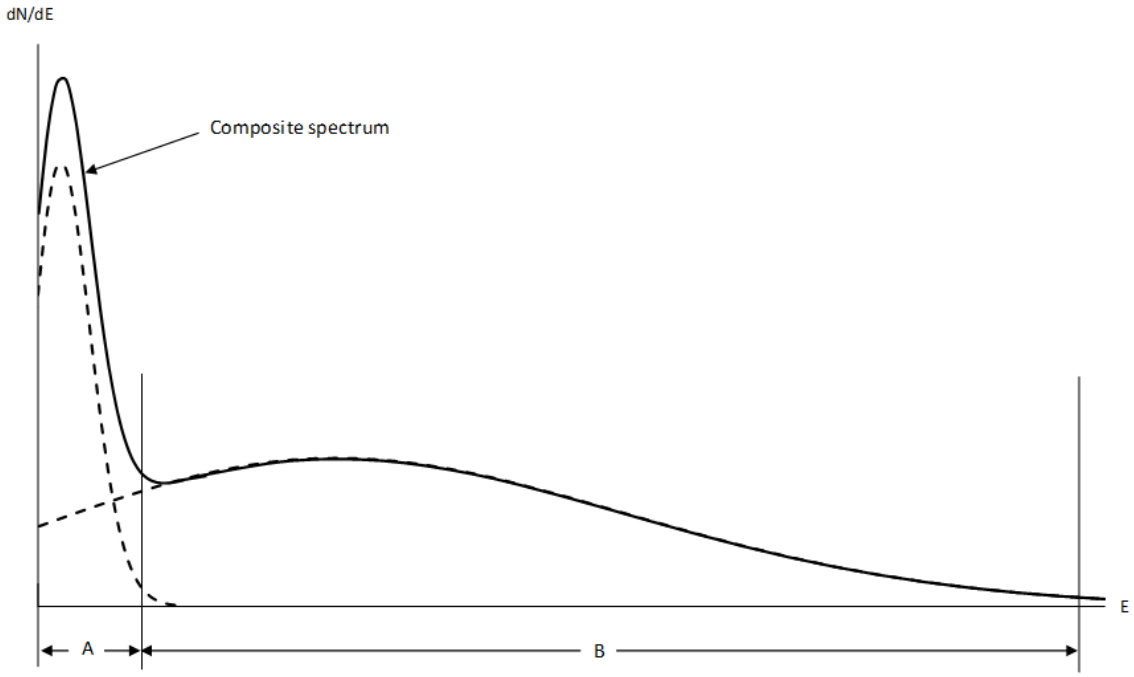

Fig. C-1: Dual label composite spectrum with counting regions A and B

In case of a mixture of two radionuclides, we have to define two energy regions in which count rates will be measured. In general, both radionuclides will contribute to the gross count rate in a region and it is necessary to calculate the difference between both contributions. In the lower energy region (denoted by "Region A") for instance, the count rate of the high energy nuclide must be subtracted from the count rate of the low energy nuclide to calculate the activity of the low energy nuclide. Therefore, it is advantageous to keep the count rate of the high energy nuclide as low as possible, or, in other words, to minimize the counting efficiency of the higher energy nuclide in Region A. This can be accomplished by lowering the upper limit of Region A. However, this results in a decrease of the measuring efficiency of the lower energy nuclide in Region A. Hence, a compromise has to be found between minimum efficiency for the higher energy nuclide and maximum efficiency for the lower energy nuclide in Region A.

We determined the H-3 and Cl-36 efficiencies for different Region A settings, by using unquenched standards and an unquenched blank: see Tab. C-1 and Fig. C-2.

Tab. C-1: H-3 and Cl-36 efficiencies for different Region A settings

Number	**Region A settings**	**H-3 efficiency** [%]	**Cl-36 efficiency** [%]
1	0 – 18.6 keV	61	7
2	0 – 16.0 keV	61	5
3	0 – 14.0 keV	61	5
4	0 – 12.0 keV	60	4
5	0 – 10.0 keV	60	3
6	0 – 8.0 keV	60	2
7	0 – 6.0 keV	57	2
8	0 – 4.0 keV	46	1
9	0 – 2.0 keV	18	0

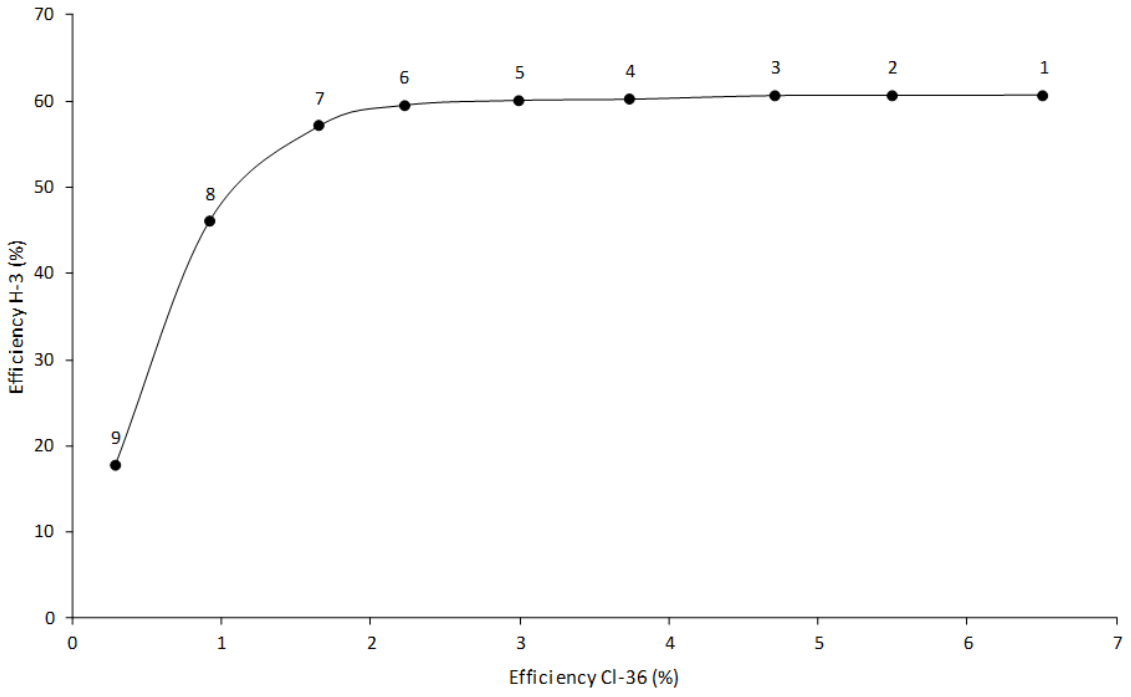

Fig. C-2: H-3 efficiency against Cl-36 efficiency for different Region A settings

As can be seen, lowering the upper limit of Region A initially results in a relatively large decrease of the Cl-36 efficiency but an insignificant decrease of the H-3 efficiency, to a certain point, where the decrease of the H-3 efficiency becomes significant. Based on these data we decided to set the Region A limits at 0 – 8.0 keV (point 6 in Fig. C-2).

As the β maximum energy of Cl-36 (709.6 keV) is much higher than the β maximum energy of H-3 (18.6 keV), it is possible to set the lower limit of the higher energy region (Region B) above the β maximum energy of H-3, meaning H-3 will not contribute to the Region B spectrum. However, raising the lower limit of Region B will result in a decrease of the Cl-36 efficiency in Region B. Therefore, we determined the Cl-36 efficiency with different Region B settings: see Tab. C-2. As can be seen, raising the lower limit to 18.6 keV (β maximum energy of H-3) results in only a 6% efficiency loss. Therefore, we decided to set the Region B limits at 18.6 – 710 keV.

Tab. C-2: Cl-36 efficiencies for different Region B settings

Region B settings	**Cl-36 efficiency** [%]
0.0 – 710 keV	105
4.0 – 710 keV	104
8.0 – 710 keV	103
12.0 – 710 keV	102
16.0 – 710 keV	100
18.6 – 710 keV	99

Investigation of the influence of quench and the ratio sample/scintillation cocktail

The matrix of the samples in the framework of the Nagra project is synthetic pore water (SPW). Because SPW contains quite high salt concentrations, quenching can occur, with efficiency loss as a consequence.

For previous routine measurements by LSC, we used a ratio sample/scintillation cocktail (Optiphase Hisafe 3 from Perkin Elmer) of 2 / 18 (to 2 mL of sample, 18 mL of scintillation cocktail was added). However, the obtain lower detection limits, it was desirable to use a ratio of 5/15 for the Nagra project.

To investigate the influence of possible quench and the suitability of a 5/15 ratio for sample/cocktail, we made 5 mL H-3 and Cl-36 standards in water and in SPW, to which 15 mL cocktail was added. These samples were examined visually and the efficiencies were determined (in the region 0 – 8.0 keV for H-3 and 18.6 – 710 keV for Cl-36).

The visual examination revealed no precipitation or flocculation after well shaking, but bubbles were noticed. However, these bubbles disappeared after one hour. Hence, in the measurement protocol (see § 8), it is included that after addition of cocktail and well shaking, one has to leave samples for a few hours before measurement.

The efficiency of H-3 is not influenced by the SPW matrix: the determined efficiency was 60% for both a standard in water and a standard in SPW (prepared with a ratio of 5/15 for sample/cocktail).

The determined efficiency of a Cl-36 standard in water was 100%, whereas it was 95% for a Cl-36 standard in SPW. This decrease of 5% in efficiency is certainly still acceptable.

Calculation of activities and uncertainties of the calculated activities

A is the total blank corrected count rate (in cpm) of the sample in Region A. It consists of the blank corrected count rates that come from the low energy nuclide and from the high energy nuclide in Region A and thus:

$$A = E_{LA} \cdot D_L + E_{HA} \cdot D_H \tag{6}$$

B is the total blank corrected count rate (in cpm) of the sample in Region B. As we have set the lower limit of Region B higher than Emax of the lower energy nuclide, it consists of only the blank corrected count rate that comes from the high energy nuclide in Region B and thus:

$$B = E_{HB} \cdot D_H \tag{7}$$

Substituting (7) in (6) gives:

$$D_L = \frac{A \cdot E_{HB} - B \cdot E_{HA}}{E_{LA} \cdot E_{HB}} = \frac{A \cdot \frac{B_H}{D_{SH}} - B \cdot \frac{A_H}{D_{SH}}}{\frac{A_L}{D_{SL}} \cdot \frac{B_H}{D_{SH}}} = \frac{(A_g - A_0) \cdot (B_g(H) - B_0) - (B_g - B_0) \cdot (A_g(H) - A_0)}{\frac{(A_g(L) - A_0) \cdot (B_g(H) - B_0)}{D_{SL}}} \tag{8}$$

Rearranging (7) gives:

$$D_H = \frac{B}{E_{HB}} = \frac{B}{\frac{B_H}{D_{SH}}} = \frac{(B_g - B_0) \cdot D_{SH}}{B_g(H) - B_0} \tag{9}$$

The standard uncertainties of DL and DH can be easily calculated by means of the spreadsheet method, by using equations (8) and (9) and the standard uncertainties of the input parameters, the calculation of which is explained below.

In general notation, a count rate is given by r = N / t, with N the total counts and t the measurement time. Because the uncertainty of t can be neglected and u(N) = √N (count measurements follow a Poisson distribution), we get:

$$u(r) = \sqrt{\frac{r}{t}}$$

By applying the above, and by the fact that the uncertainty of the activity of a standard can be neglected (see note), we get the standard uncertainties of the input parameters of equations (8) and (9):

$$u(A_g) = \sqrt{\frac{A_g}{t_{A_g}}}$$

$$u(B_g) = \sqrt{\frac{B_g}{t_{B_g}}}$$

$$u(A_0) = \sqrt{\frac{A_0}{t_{A_0}}}$$

$$u(B_0) = \sqrt{\frac{B_0}{t_{B_0}}}$$

$$u(A_g(H)) = \sqrt{\frac{A_g(H)}{t_{A_g(H)}}}$$

$$u(B_g(H)) = \sqrt{\frac{B_g(H)}{t_{B_g(H)}}}$$

$$u\left(A_g(L)\right) = \sqrt{\frac{A_g(L)}{t_{A_g(L)}}}$$

$$u(D_{SH}) = 0$$

$$u(D_{SL}) = 0$$

Notes:

- Spike solutions for the Nagra project are prepared by diluting H-3 and Cl-36 "mother standards" by weight. The uncertainty of the dilution is therefore negligible.
- For the preparation of all spike solutions, the same H-3 and Cl-36 mother standards are used. As the aim is the follow up of activities after leaching, the exact activity of the mother standards is of little importance (only the relative change of the activities in the measurement solutions is) and hence, the uncertainty of the activities of the mother standards must not be taken into account.
- By using a SPW matrix for the inlet and outlet solutions, no significant matrix changes will occur during the experiments. Furthermore, even compared to a totally unquenched standard, we saw that the SPW matrix causes no efficiency loss of H-3 and only 5% efficiency loss of Cl 36 (see § 3). Hence, an uncertainty component due to matrix effects or quenching must not be incorporated in the uncertainty of the calculated activities.

Calculation of decision thresholds

By definition, the decision threshold (D*) equals $k_{1-\alpha}$ times the standard uncertainty at zero activity (or zero net count rate):

$$D^* = k_{1-\alpha} \cdot u(D = 0)$$

Note:

- For a first kind error of 5% ($\alpha = 0.05$): $k_{1-\alpha} = 1.64$.

In Region B, we have only counts from the high energy nuclide and therefore a zero net count rate from the high energy nuclide corresponds to $B_g = B_0$. We can use the same spreadsheet calculation as we used before to get u(DH), but with setting B_g equal to B_0. This gives us $u(D_H=0)$ and thus the decision threshold for the high energy nuclide: $k_{1-\alpha}$. $u(D_H=0)$.

In Region A, with a net count rate of zero for the low energy nuclide, we do not have only a contribution form the blank/background, but also from the high energy nuclide. A high energy nuclide activity in the sample equal to D_H will give a net count rate of EHA. D_H in Region A and thus a gross count rate of:

$$A_0 + \frac{A_H}{D_{SH}} \cdot \frac{B}{\frac{B_H}{D_{SH}}} = A_0 + \frac{A_H \cdot B}{B_H} = A_0 + \frac{\left(A_g(H) - A_0\right) \cdot (B_g - B_0)}{B_g(H) - B_0}$$

We can use the same spreadsheet calculation as we used before to get $u(D_L)$, but with setting Ag equal to

$$A_0 + \frac{\left(A_g(H) - A_0\right) \cdot (B_g - B_0)}{B_g(H) - B_0}$$

This gives us $u(D_L=0)$ and thus the decision limit for the low energy nuclide: $k_{1-\alpha}$. $u(D_L=0)$.

Calculation of the recovery of several mixed Cl-36/H-3 standards

We prepared several mixed Cl-36/H-3 standards, with a ratio of the Cl-36/H-3 activities between 0.02 and 1 (corresponding to the expected ratio in measurement solutions from the Nagra project).

Recoveries (in percentage) were calculated as:

$$R\% = \frac{D}{D_{nom}} \cdot 100$$

with D_{nom} the nominal activity and D the measured/calculated activity as explained in § 4.

Note:

- The mixed standards were measured as "samples". The measured/calculated activity of H-3 is given by D_L (equation 3), the measured/calculated activity of Cl-36 is given by D_H (equation 4).

The mixed standards were prepared by gravimetrical dilution of the same mother standards as the standards used for calibration (efficiency determination). Hence, the uncertainty of Dnom must not be taken into account, leading to:

$$u(R\%) = \frac{100}{D_{nom}} \cdot u(D) \text{ or } U(R\%) = \frac{100}{D_{nom}} \cdot U(D)$$

in which u(R%) is the standard uncertainty of the recovery and u(D) is the standard uncertainty of the calculated activity, which is calculated as explained in § 4. U(R%) and U(D) are the expanded uncertainties (coverage factor of 2 is taken, giving a confidence interval of approximately 95%).

In Tab. C-2, values of D_{nom}, Cl-36 / H-3 ratios, R% and U(R%) are given for the measured mixed standards.

Tab. C-2: Values of D_{nom}, Cl-36 / H-3 ratios, R% and U(R%) for the measured mixed standards

	Nominal activity (D_{nom}) in dpm		**Ratio Cl-36/H-3 activity**	**Recovery ($R\%$) in%**		**Expanded uncertainty of $R\%$ ($U(R\%)$)**	
	H-3	**Cl-36**		**H-3**	**Cl-36**	**H-3**	**Cl-36**
Mixed standard 1	300	6.0	0.02	100.0	116.0	3.1	44
Mixed standard 2	604	18.1	0.03	99.3	101.9	2.2	16
Mixed standard 3	2'989	119	0.04	100.3	101.5	1.4	4.8
Mixed standard 4	6'010	1'180	0.2	99.8	101.4	1.4	2.1
Mixed standard 5	12'023	2'369	0.2	101.1	101.0	1.5	2.1
Mixed standard 6	17'656	6'048	0.3	101.2	100.6	1.5	1.7
Mixed standard 7	23'660	9'035	0.4	100.8	101.0	1.5	1.7
Mixed standard 8	6'028	6'024	1.0	100.9	100.0	1.7	1.4

From Tab. C-2, it is clear that all recoveries deviate from 100% by less than the expanded uncertainty of the recovery (in other words, the 95% confidence interval of each recovery includes 100%). This confirms the uncertainty calculations given in § 4, and it also justifies our assumptions that uncertainties of gravimetrical dilutions and the uncertainties of the nominal activities of the mother standards can be neglected (as these uncertainties were not included in the uncertainties of R%).

Defining measurement time

The software of the LSC allows setting only one measurement time for all regions and all samples have to be measured by the same software protocol.

We calculated the decision threshold for different measurement times, according to § 5, for a sample with no H-3 and no Cl-36 (thus, by setting $A_g = A_0$ and $Bg = B_0$). Results can be found in Tab. C-3.

Note:

- For H-3, this gives the "best" attainable decision threshold, as the H-3 decision threshold is dependent on the Cl-36 activity (the lowest H-3 decision threshold is obtained when the Cl-36 activity is zero).

Tab. C-3: Decision thresholds for a sample with no H-3 and no Cl-36, with different measurement times

Measurement time [minutes]	**Decision threshold H-3** [dpm]	**Decision threshold Cl-36** [dpm]
5	6.0	5.0
15	3.5	2.9
30	2.5	2.0
45	2.0	1.7
60	1.7	1.4

From these data, it was decided to use a measurement time of 30 minutes.

Measurement protocol

Relevant settings of the LSC software protocol (protocol number 13) are:

- measurement time: 30 minutes
- Region A: 0.0 - 8.0 keV
- Region B: 18.6 - 710 keV
- Region C: 0.0 - 18.6 keV (this region is not used for activity calculations and is just informative)

Sample preparation:

- weigh (sub)sample
- adjust to 5 mL with SPW matrix
- add 15 mL of cocktail
- shake well and leave for a few hours (bubbles must have disappeared)

Measurement sequence:

- blank (5 mL SPW + 15 mL cocktail)
- standard H-3 (5 mL standard prepared in SPW + 15 mL cocktail)
- standard Cl-36 (5 mL standard prepared in SPW + 15 mL cocktail)
- samples
- mixed standard H-3 and Cl-36 (5 mL mixed standard prepared in SPW + 15 mL cocktail)

The following standards were prepared for the measurements of samples from the Nagra project, and can be used in the measurement sequences:

- standard H-3: total activity (in 5 mL) of 6016 dpm (100.26 Bq)
- standard Cl-36: total activity (in 5 mL) of 6039 dpm (100.65 Bq)
- mixed standard: total H-3 activity (in 5 mL) of 6028 dpm (100.46 Bq) and total Cl-36 activity (in 5 mL) of 6024 dpm (100.40 Bq)

An Excel file has been made that calculates the H-3 and Cl-36 activities of the sample, the uncertainties of these calculated activities, the decision thresholds and the efficiencies.

Note:

- The mixed standard is a control standard and has to be considered/measured as a "sample".

The input parameters in the Excel file are (CPMA and CPMB are the values printed by the LSC software):

- A_g: CPMA of sample
- B_g: CPMB of sample
- $B_g(H)$: CPMB of Cl-36 standard
- $A_g(H)$: CPMA of Cl-36 standard
- $A_g(L)$: CPMA of H-3 standard
- A_0: CPMA of blank
- B_0: CPMB of blank

Quality control:

The calculated activities of the mixed standard must lie between the following limits:

- H-3: 5'950 – 6'110 dpm (99% confidence interval), and preferable 5'970 – 6'080 dpm (95% confidence interval)
- Cl-36: 5'960 – 6'090 dpm (99% confidence interval) and preferable 5'980 – 6'070 dpm (95% confidence interval)

Note:

- When a calculated activity lies not in the 99% confidence interval, the measurement series must be rejected and remeasured (eventually after taking corrective actions).

When a calculated activity lies not in the 95% confidence interval, the measurement series may be accepted, but an investigation or remeasurement is recommended. When this occurs repeatedly, corrective actions are in place.

C.2 Method

Defining region settings

The software of the gamma counter has preset region settings for the determination of Na-22: lower limit at 433 keV and upper limit at 1'417 keV. To verify the suitability of these region settings, we measured a standard and a blank with the use of these settings and with the use of a more extended region: 200 to 1'417 keV. Results are given in Tab. C-4. The value of E^2/B, which is most commonly used to optimize region settings, is higher for the preset region, which is an indication of the suitability of this region. Therefore, we will use this region for the further validation measurements and for routine measurements of samples.

Tab. C-4: Measurement of a standard of 2'805 dpm and a blank in two regions

	Region 433 – 1'417 keV	**Region 200 – 1'417 keV**
Measured cpm of standard	1'694	1'996
Measured cpm of blank (B)	122	186
% efficiency (E)	56.0	64.5
E^2/B	26	22

Investigation of matrix effect

By using a SPW matrix for the inlet and outlet solutions, no significant matrix changes are expected to occur during the experiments. Nevertheless, we compared the efficiency in water with the efficiency in a SPW matrix, by measuring a standard and a blank in water (1 mL measurement solutions, measured at lift position 3) and several standards and blanks in SPW (different volumes of measurement solutions and different lift positions, see also § 3). For the standard in water, we found an efficiency of 56.0%, and the average efficiency of standards in SPW was 54.8%. The relative difference between the efficiency in water and in SPW is thus about 2%, from which we can conclude no matrix effects will play a role (recall that comparing the matrices water and SPW is an unrealistic worst-case scenario, as all measurement solutions will have approximately the same matrix).

Investigation of measurement solution volume and lift position

Subsamples of 0.1 ml from the inlet solution of the experiments will be taken for measurement with the gamma counter and subsamples of 4 mL from the outlet.

Note:

- Initially, we intended to take one subsample of 0.2 mL from the inlet, but afterwards it was decided to take 2 subsamples of 0.1 mL. This is why we did not use 0.1 mL as the minimum volume for the tests described further, but 0.2 mL. However, because it has been proven that

the sample volume in the whole investigated range of 0.2 to 4 mL has no significant influence on the efficiency (see further), we can have confidence that a difference between 0.1 and 0.2 mL will also have no influence.

Depending on the volume of the measurement solution, the lift position for measurement must be set in the method. The manual of the gamma counter recommends the following lift positions:

0 – 0.2 mL: Lift position 1

0.2 – 0.5 mL: Lift position 2

0.5 – 1.5 mL: Lift position 3

> 1.5 mL: Lift position 4

We measured several volumes of standards and blanks (in SPW matrix), with the recommended lift positions. For the 0.2 mL solutions, which are at the "boundaries" of recommended lift positions, we used both lift positions (position 1 and 2). Results can be found in Tab. C-5.

Tab. C-5: Measurement of different volumes of standards and blanks, at the recommended lift positions

	Volume [mL]	**Lift**	**Activity** [dpm]	**Measured cpm**	**%Efficiency**
Blank 1	0.2	1	-	117	-
Standard 1	0.2	1	5'594	3'258	56.2
Blank 2	0.2	2	-	119	-
Standard 2	0.2	2	5'594	3'210	55.2
Blank 3	1	3	-	127	-
Standard 3	1	3	5'594	3'148	54.0
Blank 4	2	4	-	123	-
Standard 4	2	4	5'588	3'213	55.3
Blank 5	4	4	-	132	-
Standard 5	4	4	5'597	3'203	54.9

The possible influence of the (combined) effect of sample volume and lift position can be investigated by means of a F-test, in which the standard deviation of the measured efficiencies (for different volumes and lift positions) is compared with the expected ("theoretical") standard deviation (or standard uncertainty) of efficiencies.

The%Efficiency is given by:

$$\%E = \frac{100\ (A_S - A_0)}{D_S}$$

in which A_S is the gross count rate of a standard with activity D_S and A_0 the count rate of the blank.

Because $u(A_0)$ can be neglected compared to $u(A_S)$ and $u(D_S)$ also can be neglected (all standards are made gravimetrical from the same "mother standard"), we get:

$$u(\%E) = \frac{100}{D_S}\, u(A_S)$$

Standards were measured with a preset value for the relative uncertainty,$\%u(A_S)$, of 1% (measurement time is adjusted by the software to get a$\%u(A_S)$ of 1%). Thus:

$$u(\%E) = \frac{100}{D_S}\,\frac{\%u(A_S)}{100}\,A_S = \frac{A_S}{D_S} \approx \frac{\%E}{100} = 0.55$$

The standard deviation of the 5 measured efficiencies = stdev(56.2 ; 55.2 ; 54.0 ; 55.3 ; 54.9) = 0.78.

The F-value is thus: $F = 0.78^2 / 0.55^2 = 2.01$ and the critical value of F ($\alpha = 5\%$, $\nu_1 = 4$, $\nu_2 = \infty$) equals 2.37. This means that measuring different volumes of measurement solutions at the recommended lift positions does not result in (statistical) different efficiencies. As a consequence, for routine measurements, it is sufficient to measure only one standard with a certain volume and at a certain lift position to determine the efficiency, which can then be used for all sample measurements (samples with different volumes measured at the recommended lift positions).

Calculation of activities and uncertainties of the calculated activities

With A_g the gross count rate of the sample (in cpm), A_0 the count rate of the blank and E the efficiency, the activity D of the sample (in dpm) is given by:

$$D = \frac{A_g - A_0}{E}$$

And because $E = (A_s - A_0) / D_s$, with A_s the gross count rate of a standard with activity D_S:

$$D = \frac{(A_g - A_0)\, D_S}{A_s - A_0}$$

The standard uncertainty of D can be easily calculated by means of the spreadsheet method, by using the above equation and the standard uncertainties of the input parameters, the calculation of which is explained below.

In general notation, a count rate is given by $r = N / t$, with N the total counts and t the measurement time. Because the uncertainty of t can be neglected and $u(N) = \sqrt{N}$ (count measurements follow a Poisson distribution), we get:

$$u(r) = \sqrt{\frac{r}{t}}$$

By applying the above, and by the fact that the uncertainty of the activity of the standard can be neglected (see note), we get the standard uncertainties of the input parameters:

$$u(A_g) = \sqrt{\frac{A_g}{t_{A_g}}}$$

$$u(A_0) = \sqrt{\frac{A_0}{t_{A_0}}}$$

$$u(A_S) = \sqrt{\frac{A_S}{t_{A_S}}}$$

$$u(D_S) = 0$$

Notes:

- Spike solutions for the Nagra project are prepared by diluting a Na-22 "mother standard" by weight. The uncertainty of the dilution is therefore negligible.
- For the preparation of all spike solutions, the same mother standard is used. As the aim is the follow up of activities after leaching, the exact activity of the mother standard is of little importance (only the relative change of the activities in the measurement solutions is) and hence the uncertainty of the activity of the mother standard must not be taken into account.
- By using a SPW matrix for the inlet and outlet solutions, no significant matrix changes will occur during the experiments. Furthermore, even compared to a standard in water, we saw that the SPW matrix causes no efficiency loss or rise. Hence, an uncertainty component due to matrix effects must not be incorporated in the uncertainty of the calculated activities.

Defining measurement time and decision threshold

By definition, the decision threshold (D^*) equals $k_{1-\alpha}$ times the standard uncertainty at zero activity (or zero net count rate):

$$D^* = k_{1-\alpha} \cdot u(D = 0)$$

Note:

- For a first kind error of 5% ($\alpha = 0.05$): $k_{1-\alpha} = 1.64$.

We can use the same spreadsheet calculation as mentioned in § 4 and setting $A_g = A_0$ to get u(D=0) and the decision threshold $k_{1-\alpha}$. u(D=0). We calculated the decision threshold for different measurement times (with the use of A_0 = 132 cpm, A_S = 3'203 cpm and D_S = 5'597), the results of which are given in Tab. C-6.

Tab. C-6: Decision threshold for different measurement times

Measurement time [min]	**Decision threshold** [dpm]
5	22
15	13
30	9
45	7
60	6

Based on these data, it was decided to take a measurement time of 30 minutes.

Measurement protocols

Relevant settings of the measurements protocols:

1. Protocol #1 for 0.1 - 0.2 mL measurement solutions
   - measurement time: 30 minutes
   - 1Sigma%: 1%
   - Region A: 433 – 1'417 keV
   - lift position: 1
2. Protocol #24 for 2 - 4 mL measurement solutions
   - measurement time: 30 minutes
   - 1Sigma%: 1%
   - Region A: 433 - 1417 keV
   - lift position: 4

Measurement sequence:

1. Protocol #1
   - blank 0.2 mL SPW (vial "B3")
   - standard 0.2 mL in SPW (vial "S3")
   - samples from inlet
2. Protocol #24
   - samples from outlet
   - blank 4 mL SPW (vial "B5")
   - standard 4 mL in SPW (vial "S6")

Note:

- The 4 mL blank and standard are a control blank and standard.

An Excel file has been made that calculates the Na-22 activities of the samples, the uncertainties of these calculated activities and the decision thresholds.

The input parameters in the Excel file are:

- date of measurement
- CPMA and measurement time (in minutes) of the calibration blank (vial "B3")
- CPMA and measurement time (in minutes) of the calibration standard (vial "S3")
- name, CPMA and measurement time (in minutes) of the samples

Remark: The control blank (vial "B5") and the control standard (vial "S6") are measured as "samples". As "sample names" can be given in "control blank" and "control standard".

Quality control

The calculated activities of the control blank and control standard must lie between the following limits:

- control blank: between -20 en 20 dpm
- control standard: activity limits depend on measurement date:

Date of measurement	**Lower limit** [dpm]	**Upper limit** [dpm]
January 2021	4'950	5'950
February 2021	4'850	5'850
March 2021	4'750	5'700
April 2021	4'650	5'600

When the measured activity of the control blank or control standard does not lie in the above-mentioned intervals, the measurement series must be rejected and remeasured (eventually after taking corrective actions).

Appendix D: Model approach SCK CEN

D.1 General

The model approach needed for a certain experimental situation depends on the conditions of the experiment, i.e. variable or constant concentration at the in- and/or outlet. SCK CEN developed different models reflecting different conditions that occur in a Through-Diffusion experiment: "fit36" is used for a constant tracer concentration at the inlet (high concentration C_0 (1/m^3)) and a (constant) zero (tracer) concentration at the outlet is "fit36" while "fit36_C0_var" is used in case that the inlet concentration is variable (as is the case in the conducted experiments)).

In both fit36 and fit36_C0_var a constant zero outlet concentration is assumed. This approximation is valid in case that the outlet (tracer) concentration is much lower than the inlet concentration in the experiment. This condition can be achieved in case of a very large outlet volume or, as done in the present experiments, by regularly replacing the outlet volume by a new tracer free outlet volume.

Also, the filters at in- and outlet side need to be taken up in the model. The numerical model "dfit36_varC0_V3_met_filters_weak" takes into account diffusion through the filters (with continuous boundary conditions, meaning flux conservation and concentration conservation, at the clay/filter boundaries). In this model approach the inlet and outlet filters are assumed identical (same thickness, same value of the diffusion parameters). For the filter diffusion parameters, three options are available:

- Option 1: F=C (Filter is Clay) the values of the diffusion parameters for the filters and the clay are the same
- Option 2: FF (Fixed Filter) the values of the diffusion parameters of clay and filters are independent from each other
- Option 3: FηR: the values of apparent diffusion coefficients of clay and filters are equal and the values of the capacity factor ηR (reducing to the accessible porosity in case of unretarded tracers like HTO and chloride) are independent of each other

Some justification and extra comments concerning these options:

- Option 1: F=C: if filters and clay have (nearly) the same properties, the model reduces to "fit36_C0_var". This allows a numerical verification with the analytical fit36_C0_var solution.
- Option 2: this is the general option, with four transport parameters: apparent diffusion coefficient D_a (m^2/s) and capacity factor ηR (-) (with η the accessible porosity (-) and R (-) the retardation factor, R = 1 for HTO and chloride) for the clay and for the filters. Fitting four parameters from both inlet concentration evolution vs. time and outlet concentration evolution vs. time, leads to strong correlations between these parameters and hence less reliable parameter values. A better strategy is to determine the diffusion parameters of the filters separately, and fix them as a constant when fitting the experimental data to obtain the values of the clay diffusion parameters (only 2 parameters are fitted). This option is called Fixed Filter (FF). The problem here is to obtain representative parameters for the filters. TD experiment can be done on a stack of filters and can indeed provide transport parameters for the filters, but in case of experiments where clays are confined between filters clay particles enter the filter, due to the swelling of the clay, and modify its diffusion parameters. This means that this is not constant for each experiment. This has clearly been demonstrated by Aertsens et al. (2011, 2017) for Sr diffusion in Boom Clay.

- Option 3: Experimentally we have measured the diffusion parameters of the filters for HTO and for strontium, but not for anions. As these filters have no charged surface, the effect of electric double layers is negligible and the accessible porosity in these filters will be equal for cations, anions and neutral species. As such the porosity measured for HTO can be used for anions. Because the anion apparent diffusion coefficient in the filters is not experimentally determined, it is assumed equal to that of the clay.

D.2 Influence of filters in the diffusion experiments: comparing F=C (Filter = Clay) to FF (Fixed Filter)

The experiments are fitted with both the F=C and the FF option. Here we derive an approximate relation for the effective diffusion coefficients of the clay core derived by both ways of fitting.

Since the inlet volume is sufficiently large, the concentration decrease during the experiment is relatively slow (with respect to the evolution of the outlet concentration) and near the end of the experiments an approximately stationary state is reached. Evidently, this is an approximation: at extremely large times all concentrations in the system are zero.

In this approximately stationary state, for the F=C case, the diffusive flux J (1/ (m^2 s)) through the system (clay + filters) is

$$J = D_{eff} \frac{\Delta C}{L_{tot}} \tag{10}$$

with D_{eff} (m^2/s) the effective (overall) diffusion coefficient, ΔC the inlet concentration (1/m^3) and L_{tot} (m) the total system length

$$L_{tot} = L_C + L_F \tag{11}$$

with L_C (m) the clay core thickness and L_F (m) the total filter thickness (twice the thickness of an individual filter).

For the FF case, substituting expression (10) in

$$\Delta C_{tot} = \Delta C_C + \Delta C_F \tag{12}$$

with ΔC_C the concentration difference over the clay core and ΔC_F the concentration difference over the total filter thickness, leads to

$$\frac{L_{tot}}{D_{eff}} = \frac{L_F}{D_{eff,F}} + \frac{L_C}{D_{eff,C}} \tag{13}$$

with $D_{\text{eff,F}}$ (resp. $D_{\text{eff,C}}$) the effective diffusion coefficient of the filter (resp. clay).

The previous expression can be transformed in

$$\frac{D_{eff}}{D_{eff,C}} = \frac{1}{\frac{D_{eff,C}}{D_{eff,F}}\frac{L_f}{L_{tot}} + \left(1 - \frac{L_f}{L_{tot}}\right)} \tag{14}$$

It is evident for longer clay cores (lower ratio L_f/L_{tot}) that the influence of the filters decreases ($D_{eff}/D_{eff,C} \rightarrow 1$). For the filters used at SCK CEN is $L_F = 2$ mm and for HTO $D_{app,F} \approx 3.5\ 10^{-10}$ m^2/s and $\eta_F \approx 0.4$ (retardation factor R =1) (Aertsens et al., 2011), leading to $D_{eff,F} = \eta_F\ D_{app,F} = 1.4\ 10^{-10}$ m^2/s.

D.3 How to fit: absolute and relative fits

By fitting, one tries to determine parameter values with the aim that for some function *f(x,P)* (with x a variable and P a parameter), the set $f(x_i,P)$ (where the index i varies between one and the number of points N) is as close as possible to a set of values (x_i,y_i).

A possible way to do this is to minimize (by varying the parameter P) the function χ^2, defined by

$$\chi^2 = \sum_{i=1}^{N}\left(f(x_i,P) - y_i\right)^2 \tag{15}$$

The value of the parameter P where the function χ^2 is minimal is then considered as the best estimate for the parameter P.

A disadvantage of using the fit function (15) is that points with a large value y_i (or $f(x_i,P)$) dominate the function χ^2. Hence, the influence of points with a small y_i (or $f(x_i,P)$) value on the optimal value for the parameter P is nearly zero. We illustrate this by a simple example, in which we fit only two points: a point (x_1, $y_1 = 100$) and a point (x_2, $y_2 = 0.1$). Suppose that for both points the function *f(x,P)* lies around 90% of the y-values for the relevant P-values. Hence the contribution of the point x_1 in the χ^2 function () is approximately $(100 - 90)^2 = 100$. Similarly, the contribution of the second point x_2 is approximately $(0.1 - 0.09)^2 = 0.0001$. Since one has to minimize the sum of both contributions, it is very obvious that the minimum of the function χ^2 will be determined almost exclusively by the point x_1.

This problem can be remedied by taking another function χ^2, for instance

$$\chi^2 = \sum_{i=1}^{N}\left(\frac{f(x_i,P) - y_i}{y_i}\right)^2 \tag{16}$$

With this definition of the function χ^2, the contribution of both points of the previous example is similar because $((100 - 90)/100)^2 = ((0.1 - 0.09)/0.1)^2$. So, in this case, both points will really determine the optimal value of the parameter P. Because in (16), we normalize all points to a value around one, we call fits using this χ^2 function "relative fits". Similarly, fits using the function () can be called "absolute fits".

Since both fit functions (15) and (16) will lead to a different optimal value for the parameter P, an evident question is, which of both fit functions, (15) or (16), is the most appropriate as they are both valid. Like for choosing a function $f(x,P)$, it is up to the person performing the fit to make a choice for the function χ^2. Obviously, the optimal values clearly depend on both choices (for χ^2 and for $f(x,P)$). However, in general, if the fit function $f(x_i,P)$ agrees well with the values y_i, then both choices of χ^2 presented here lead to similar optimal values for the parameter P. If this agreement is not so good, then the optimal values obtained by both functions χ^2 presented here are probably not similar. However in that case, these optimal values are not very reliable either.

The (root) Mean Squared Error of the fits (MSE) is

$$MSE = \sqrt{\frac{\chi^2}{N - N_P}} \tag{17}$$

with N_p the number of parameters in the fit.

Appendix E: Diffusion experiments at SCK CEN

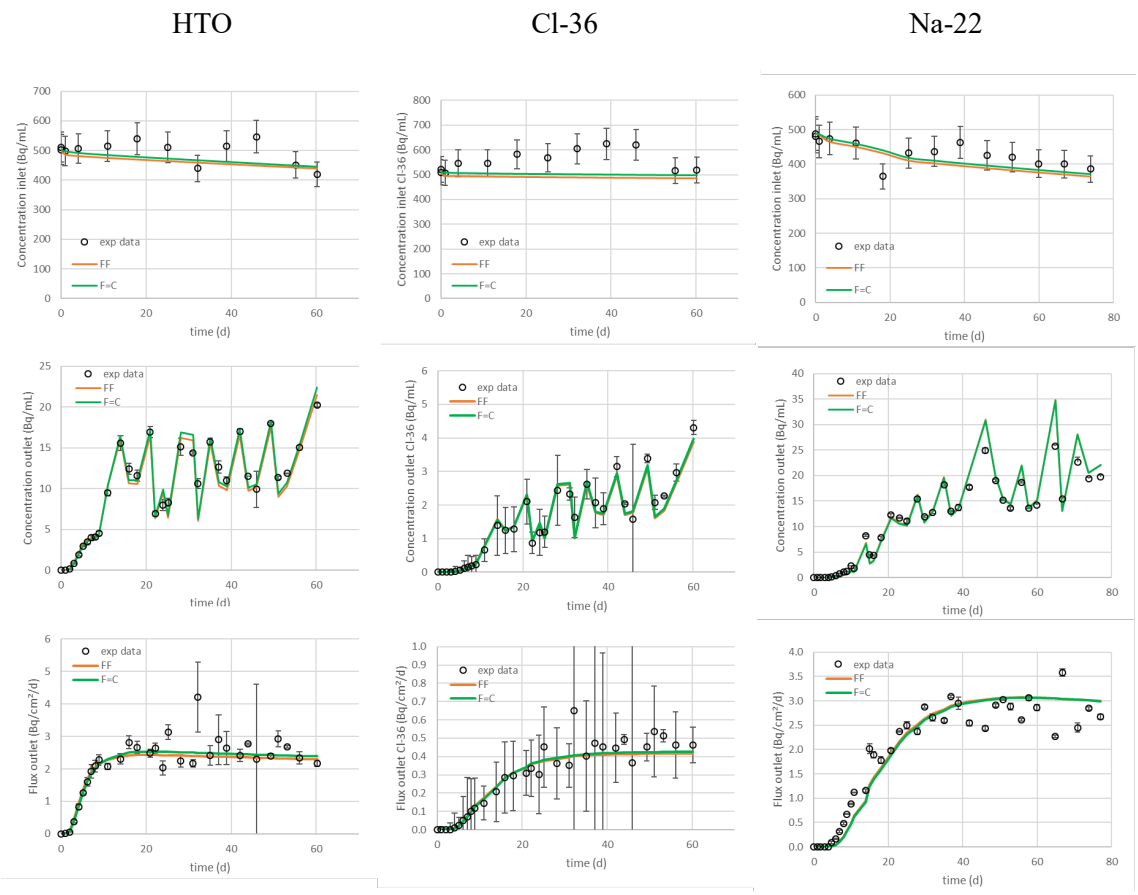

Fig. E-1: Experimental data (points) and fits (FF orange line, F=C green line) of sample core TRU1-1-882.36-DI of HTO, Cl-36 and Na-22 diffusion show (i) the evolution of the inlet concentration (Bq/mL), (ii) the evolution of the outlet concentration (Bq/mL) and (iii) the evolution of the outlet flux (Bq/cm²/d)

HTO Cl-36 Na-22

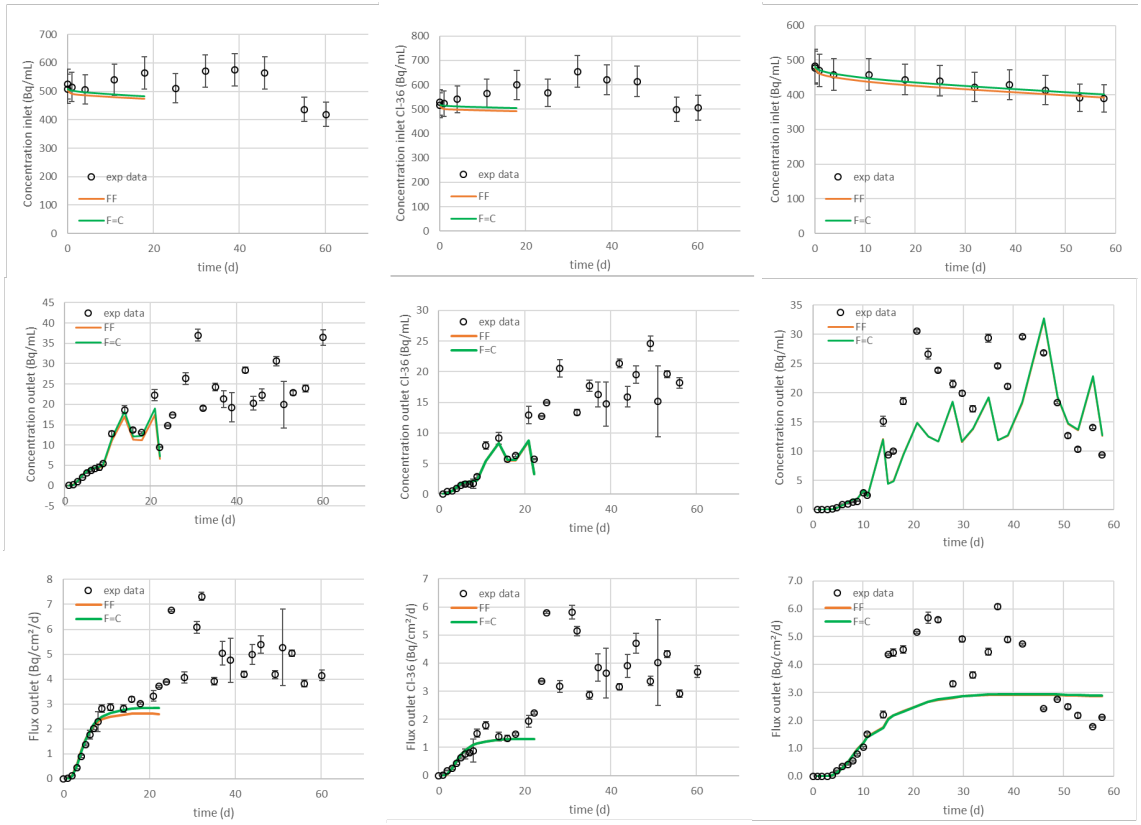

Fig. E-2: Experimental data (points) and fits (FF orange line, F=C green line) of sample core TRU1-1-890.39-DI of HTO, Cl-36 and Na-22 diffusion show (i) the evolution of the inlet concentration (Bq/mL), (ii) the evolution of the outlet concentration (Bq/mL) and (iii) the evolution of the outlet flux (Bq/cm²/d)

HTO Cl-36 Na-22

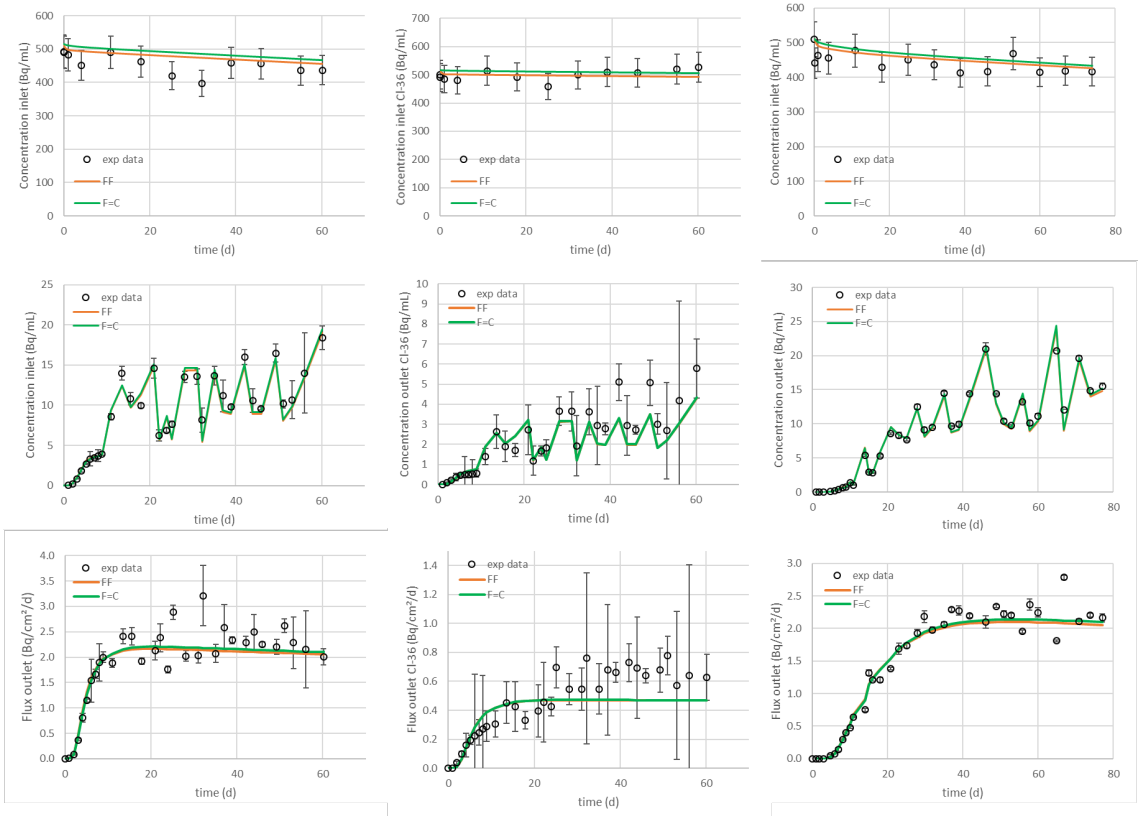

Fig. E-3: Experimental data (points) and fits (FF orange line, F=C green line) of sample core TRU1-1-902.85-DI of HTO, Cl-36 and Na-22 diffusion show (i) the evolution of the inlet concentration (Bq/mL), (ii) the evolution of the outlet concentration (Bq/mL) and (iii) the evolution of the outlet flux (Bq/cm²/d)

HTO Cl-36 Na-22

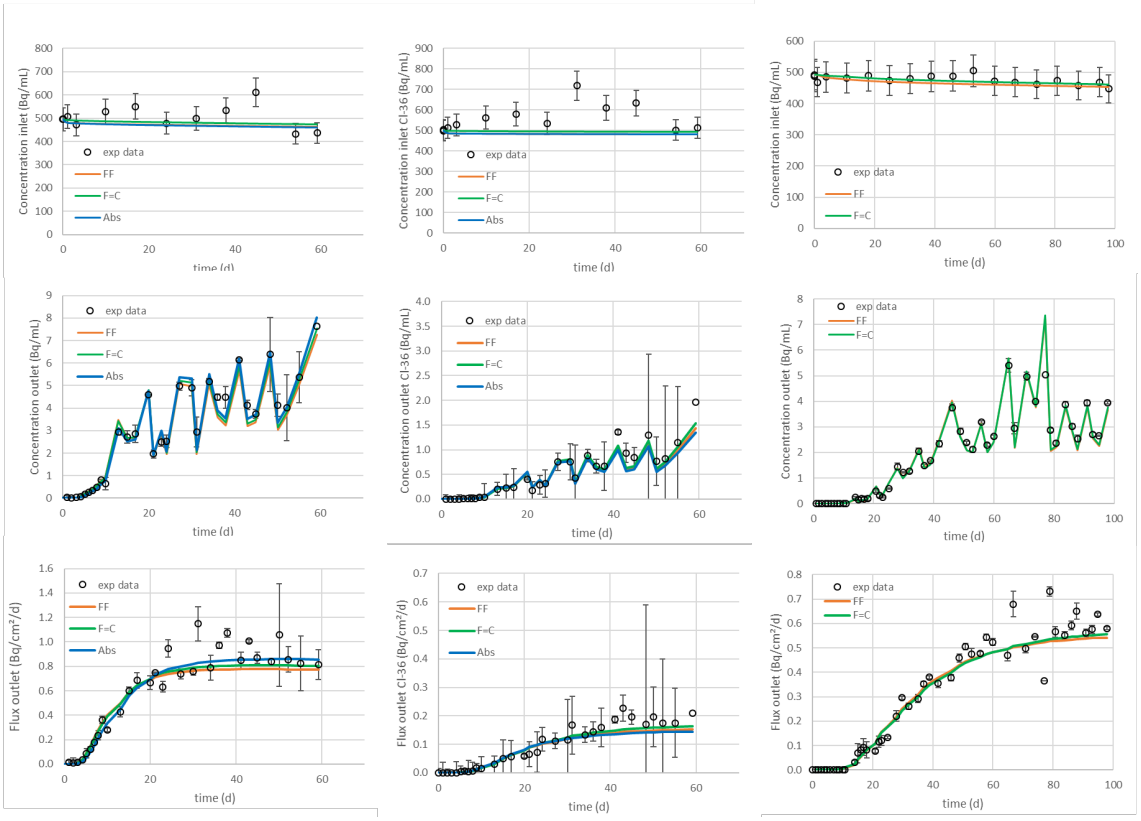

Fig. E-4: Experimental data (points) and fits (FF orange line, F=C green line, Abs blue line) of sample core TRU1-1-938.90-DI of HTO, Cl-36 and Na-22 diffusion show (i) the evolution of the inlet concentration (Bq/mL), (ii) the evolution of the outlet concentration (Bq/mL) and (iii) the evolution of the outlet flux (Bq/cm²/d)

For HTO and Cl-36 also the results of the absolute fit are shown.

Appendix F: Diffusion experiments at PSI-LES

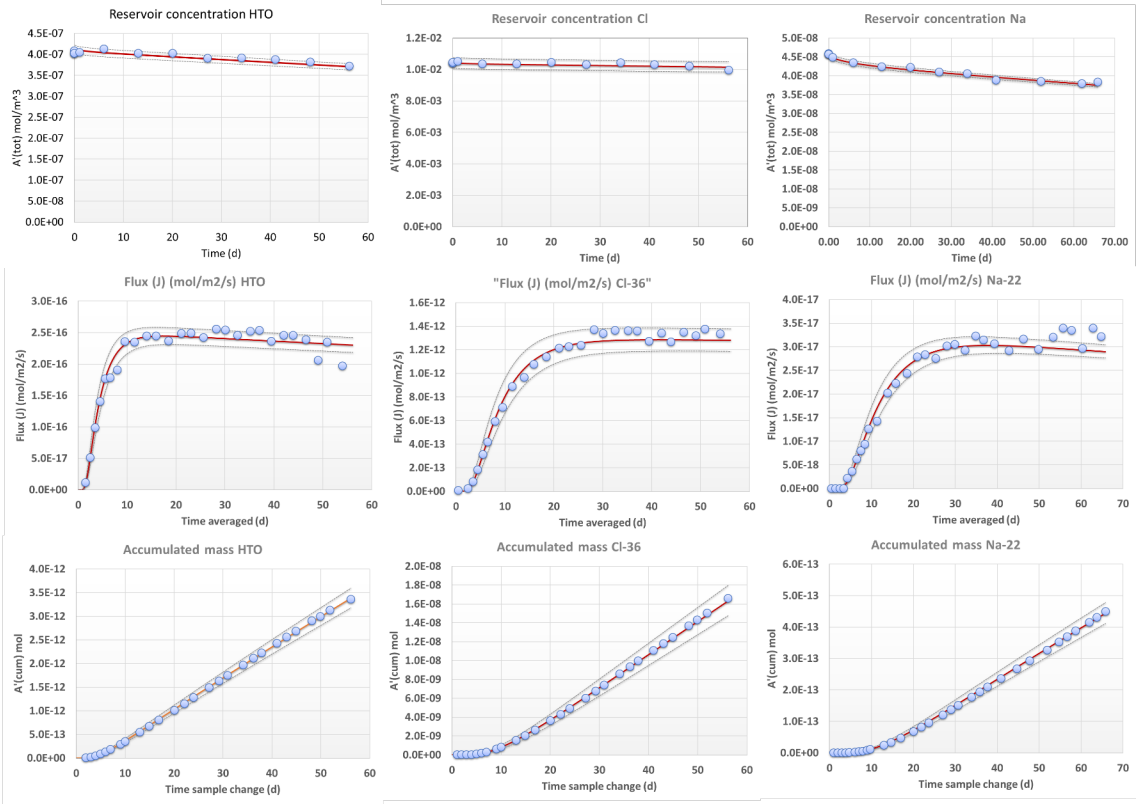

Fig. F-1: Experimental data (points) and fits (line) of sample core TRU1-870.23-S1 of HTO, Cl-36 and Na-22 diffusion show (i) the evolution of the inlet concentration (mol/m³), (ii) the evolution of the outlet flux (mol/m²/s) and (iii) the accumulated mass in the outlet (mol)

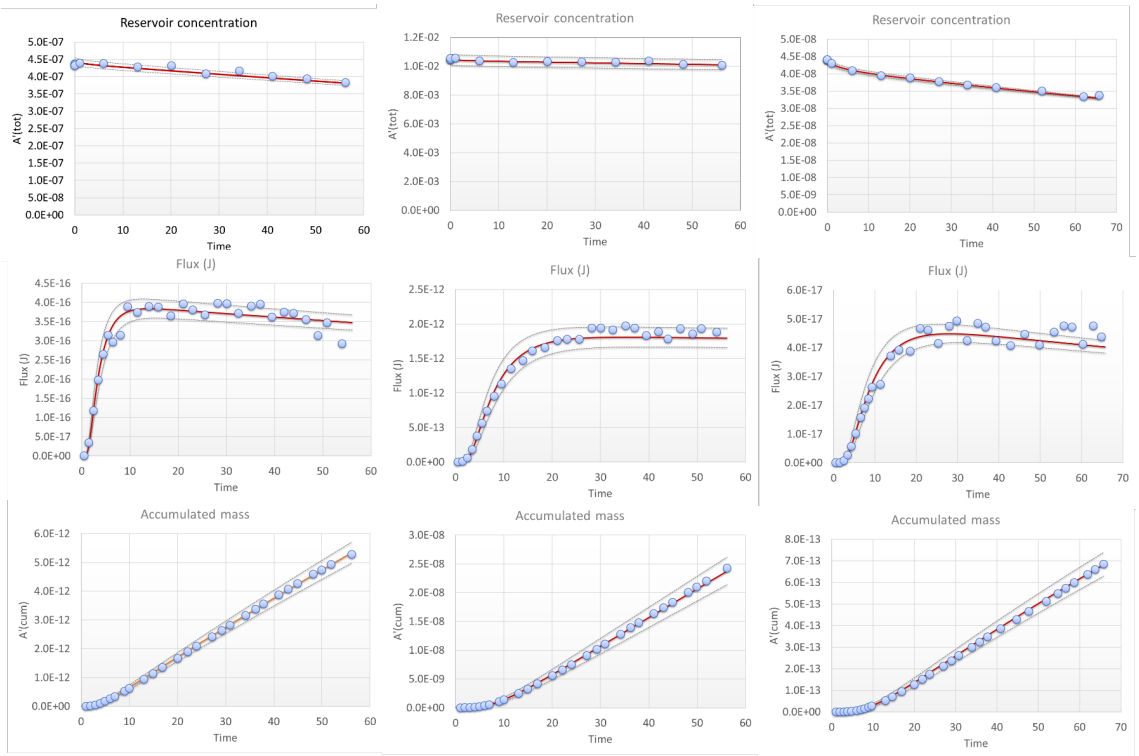

Fig. F-2: Experimental data (points) and fits (line) of sample core TRU1-1-882.36-DI HTO, Cl-36 and Na-22 diffusion show (i) the evolution of the inlet concentration (mol/m³), (ii) the evolution of the outlet flux (mol/m²/s) and (iii) the accumulated mass in the outlet (mol)

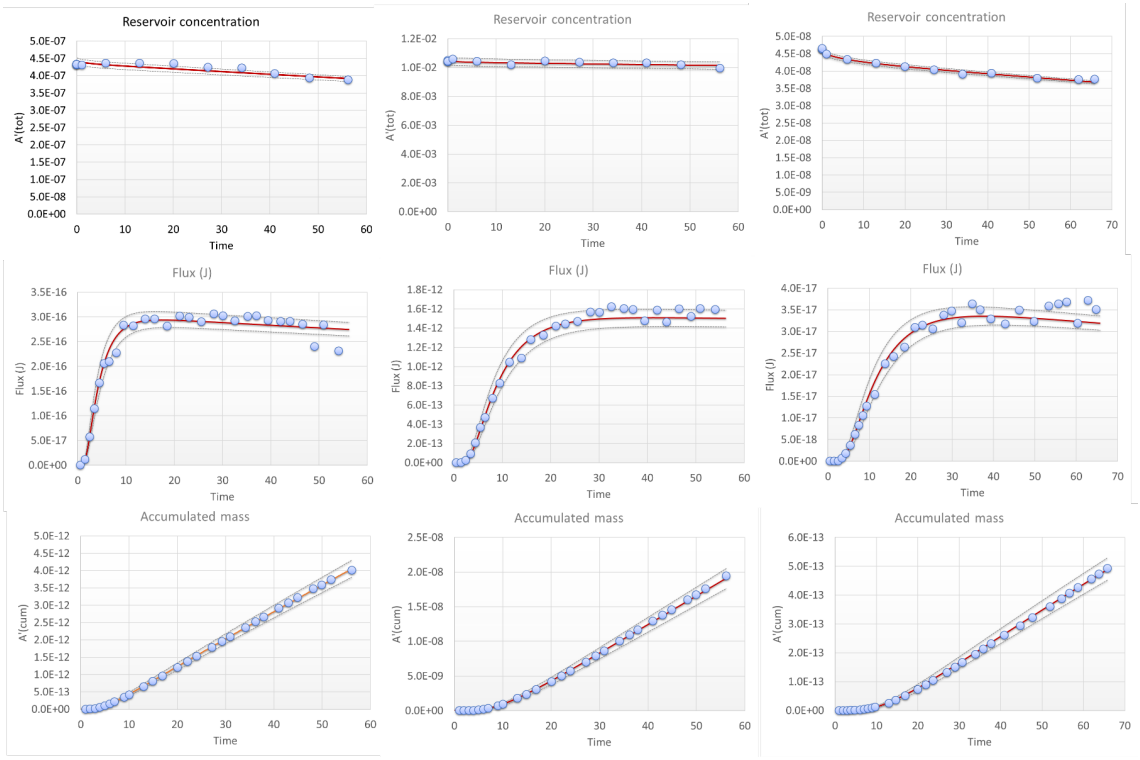

Fig. F-3: Experimental data (points) and fits (line) of sample core TRU1-1-890.39-DI of HTO, Cl-36 and Na-22 diffusion show (i) the evolution of the inlet concentration (mol/m³), (ii) the evolution of the outlet flux (mol/m²/s) and (iii) the accumulated mass in the outlet (mol)

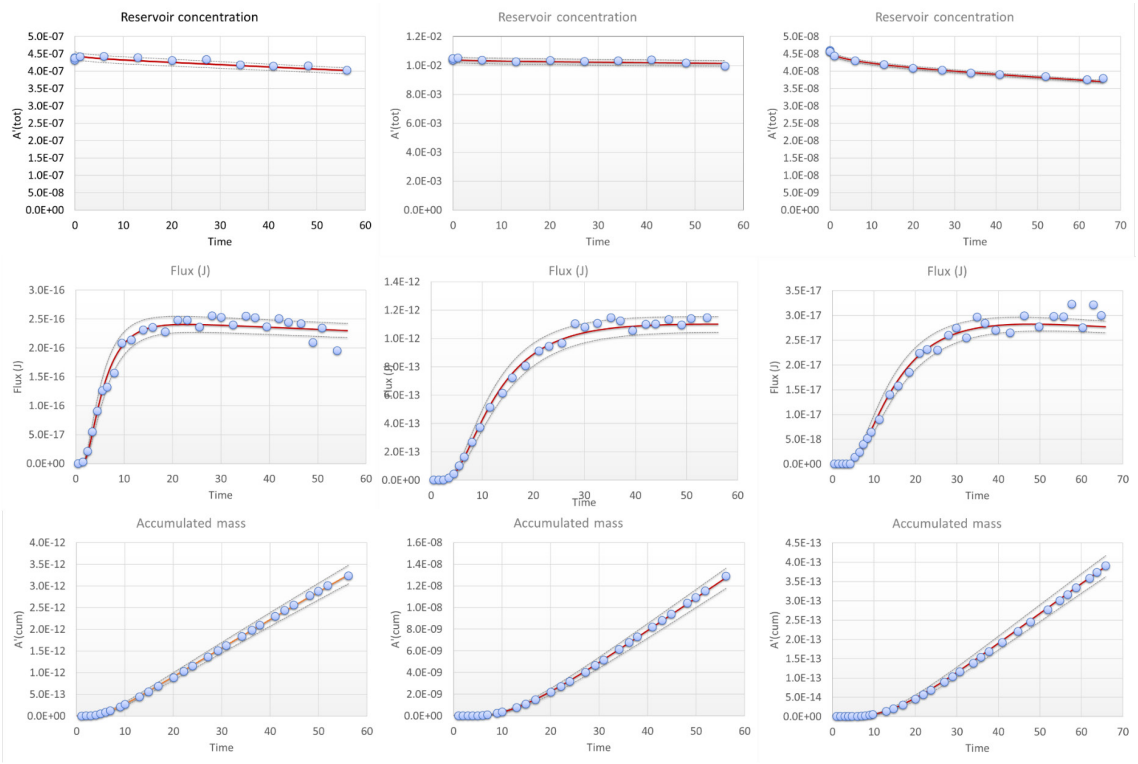

Fig. F-4: Experimental data (points) and fits (line) of sample core TRU1-1-902.85-DI of HTO, Cl-36 and Na-22 diffusion show (i) the evolution of the inlet concentration (mol/m³), (ii) the evolution of the outlet flux (mol/m²/s) and (iii) the accumulated mass in the outlet (mol)

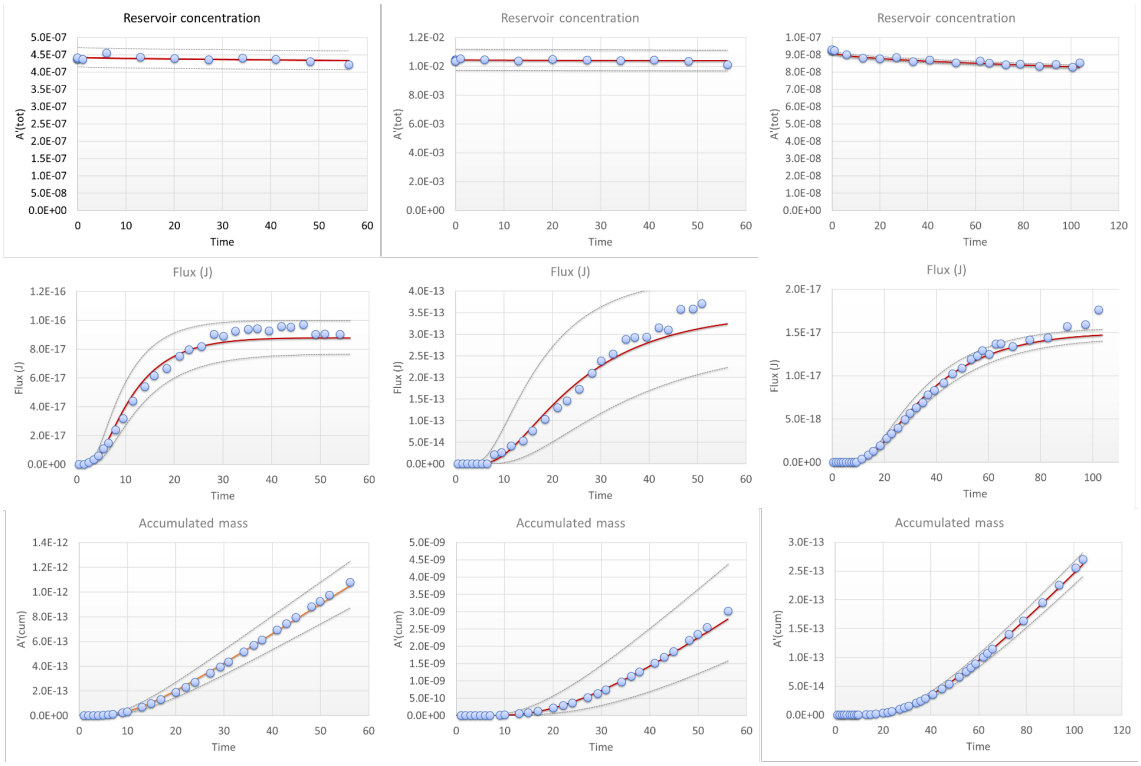

Fig. F-5: Experimental data (points) and fits (line) of sample core TRU1-1-938.90-DI of HTO, Cl-36 and Na-22 diffusion show (i) the evolution of the inlet concentration (mol/m³), (ii) the evolution of the outlet flux (mol/m²/s) and (iii) the accumulated mass in the outlet (mol)

Appendix G: Overview diffusion parameters from SCK CEN and PSI-LES (HTO and Cl-36)

Tab. G-1 gives the parameters of the independent studies (as given in Part 2 and 3) and the results of the modelling benchmark exercise (model approaches of both institutes on each other datasets). For the fits of SCK CEN, D_a and ηR are the fitted parameters (and D_e calculated), while in the approach of PSI-LES D_e and ηR are the fitted parameters and D_a is calculated by dividing D_e with ηR.

Tab. G-1: Comparison of the diffusion parameters of HTO and Cl-36 obtained from the datasets from SCK CEN and PSI-LES.

Each dataset was fitted with the model approach of each institute.

Sample	**Exp data**	**Fit**		**HTO**			**Cl-36**		
				$D_a \times 10^{-11}$ [m^2/s]	**η** [-]	**$D_e \times 10^{-12}$** [m^2/s]	**$D_a \times 10^{-11}$** [m^2/s]	**η** [-]	**$D_e \times 10^{-12}$** [m^2/s]
TRU1-1-870.23-DI	SCK	PSI SCK	Average F=C FF						
	PSI	 PSI SCK	Min. Max. Average F=C	 8.48	0.114 0.128 0.121 0.108	7.40 7.88 7.64 9.16	 4.14	0.050 0.056 0.053 0.045	2.47 2.61 2.54 1.85
TRU1-1-882.36-DI	SCK	PSI SCK	Average F=C FF	6.97 10.80 7.62	0.035 0.101 0.111	9.38 10.90 8.46	2.62 4.34 2.74	0.054 0.041 0.050	1.41 1.76 1.37
	PSI	 PSI SCK	Min. Max. Average F=C	 11.80	0.125 0.143 0.134 0.122	11.80 12.80 12.30 14:40	 5.40	0.056 0.064 0.060 0.052	2.27 2.47 2.37 2.81
TRU1-1-890.39-DI	SCK (21 days)	PSI SCK	Average F=C FF	6.18 10.40 7.13	0.158 0.110 0.117	9.76 11.40 8.34	7.06 10.80 6.67	0.061 0.047 0.059	4.31 5.03 3.96
	PSI	 PSI SCK	Min. Max. Average F=C	 9.48	0.121 0.137 0.129 0.118	9.13 9.75 9.44 11.20	 4.69	0.055 0.061 0.058 0.050	1.91 2.05 1.98 2.35
TRU1-1-902.85-DI	SCK	PSI SCK	Average F=C FF	6.23 10.30 6.65	0.117 0.082 0.099	7.27 8.50 6.56	5.89 8.93 5.32	0.021 0.020 0.026	1.21 1.77 1.37
	PSI	 PSI SCK	Min. Max. Average F=C	 7.80	0.127 0.141 0.134 0.122	7.81 8.33 8.07 9.52	 3.60	0.056 0.060 0.058 0.050	1.49 1.57 1.53 1.79
TRU1-1-938.90-DI	SCK	PSI SCK	Average F=C FF	2.52 4.73 2.98	0.122 0.070 0.084	3.08 3.32 2.51	1.59 2.37 1.48	0.029 0.029 0.033	0.453 0.675 0.490
	PSI	 PSI SCK	Min. Max. Average F=C	 4.40	0.083 0.101 0.092 0.077	2.74 3.16 2.95 3.40	 1.96	0.027 0.043 0.035 0.029	0.486 0.500 0.493 0.572